UCSF
UC San Francisco Electronic Theses and Dissertations

Title
Chd1 is essential for the emergence of definitive hematopoietic stem and progenitor cells

Permalink
https://escholarship.org/uc/item/15j77943

Author
Koh, Fong Ming

Publication Date
2014

Peer reviewed|Thesis/dissertation

eScholarship.org Powered by the California Digital Library
University of California

Chd1 is essential for the emergence of definitive hematopoietic stem and progenitor cells

by

Fong Ming Koh

DISSERTATION

Submitted in partial satisfaction of the requirements for the degree of

DOCTOR OF PHILOSOPHY

in

Biomedical Sciences

in the

GRADUATE DIVISION

of the

UNIVERSITY OF CALIFORNIA, SAN FRANCISCO

Copyright 2014

by

Fong Ming Koh

To Jasmine,

for your enduring support and companionship

over the past 10 years.

This long journey would have been unbearable

without your presence.

And to baby Timothy,

born 15 Dec 2014,

marking the start of a new chapter in my life.

Acknowledgments

This thesis is the culmination of work conducted over the past 5 years in the laboratory of Miguel Ramalho-Santos. The project started with a planned focus to investigate the role of Chd1 on early embryonic and primordial germ cell development. The initial excitement when I found TNAP-Cre; $Chd1^{flox/-}$ mutants to be embryonic lethal soon led to confusion due to the unexpected phenotype, and the project took several unexpected turns before ending up in its current form as a thesis on hematopoiesis. Throughout this process, Miguel has consistently provided me with the freedom and resources to pursue any ideas I deemed feasible. His hands-off approach to mentorship, coupled with his constant availability to provide advice and support when I struggled, has provided me with the latitude to develop as an independent thinker. In addition, his patience and persistence in pushing the project through to its logical end, despite going well out of his field of expertise, is admirable and this will shape how I handle projects in the future.

My research experience was enriched by my colleagues, colloquially termed Santos Lab 2.0. Fellow graduate students, Bea, Mike and Kathryn, made the daily struggles less lonely. I have worked closely with two wonderful post-docs, Marcela and Lance, on their projects on Chd1 and Hira respectively, and their insights have helped me gain perspective on my own projects. Lab manager Laure served commendably as an enthusiastic lab party planner. Priscilla was initially hired to manage my rapidly

expanding mouse colony, but went beyond and contributed significantly to multiple aspects of this project.

UCSF is truly a great place to do collaborative science. Many PIs were willing to open their doors when I had little more than vague hypotheses for a strange embryonic phenotype, and they have graciously allowed me to go fishing for ideas in their vast sea of collective wisdom. My thesis committee members, Barbara and Benoit, served as a counterweight to the various half-baked ideas we had come up with and helped to focus the project on the most logical route towards graduation.

I am fortunate to be surrounded by loving friends and family outside of lab. The small community of Singaporeans in the city has provided much joy and laughter to neutralize the frustrations and disappointments associated with research. Yun, Jiamin and Sarah have been partners in many weekend adventures; Albert and Marta partook in whining sessions on graduate school life; Peirong and Xinzi kept the smiles on our faces at all times; and Jean led the way to many food-induced comas.

Both my parents and in-laws have been very supportive of our extended stay far from home. While I regret being absent from the formative years of my baby sister, Maggie, I look forward to spending some quality time with her after my graduation.

Most importantly: Jasmine, my best friend, companion and wife. We had spent the last decade traveling the world in search of the grandest sights and the finest foods. I can't imagine a better partner to spend the next decade with, building a new life and a new home together.

Contributions to thesis work

Chapter 1 is adapted from a review article published in the journal, Current Opinion in Genetics & Development, and was written under the supervision of Miguel Ramalho-Santos. Michael Sachs and Marcela Guzman-Ayala contributed writing to several sections of the manuscript. (Koh, F. M., Sachs, M., Guzman-Ayala, M. and Ramalho-Santos, M. (2010). Parallel gateways to pluripotency: open chromatin in stem cells and development. Curr Opin Genet Dev 20, 492–499. doi: 10.1016/j.gde.2010.06.002)

Chapters 2 and 3 are adapted from a research article that has been submitted for publication, and was done under the supervision of Miguel Ramalho-Santos. This project was a collaboration with Ann Zovein and her lab members, Carlos Lizama and John Hawkins. Priscilla Wong managed the mouse colony under my supervision, performed genotyping and assisted with experiments. Carlos Lizama and John Hawkins conducted immunostainings, methylcellulose colony-formation assays and OP9-DL1 assays on E10.5 AGMs.

Chd1 regulates the emergence of definitive hematopoietic stem and progenitor cells

by Fong Ming Koh

Abstract

Lineage specification during development involves reprogramming of transcriptional states, but little is known about how this is regulated in vivo. We recently found that the chromatin remodeler Chd1 promotes a globally elevated transcriptional output in mouse embryonic stem cells and is essential for epiblast development. Here we report that Chd1 regulates the emergence of hematopoietic progenitors from the endothelium of embryonic blood vessels. Endothelial-specific deletion of *Chd1* using *Tie2-Cre* leads to embryonic lethality by E15.5. Mutant embryos have apparently normal vasculature but show signs of anemia as early as E11.5, are depleted of definitive hematopoietic stem and progenitor cells, and display a complete failure of fetal liver erythropoiesis. At E10.5, mutants are morphologically indistinguishable from controls and contain normal numbers of intra-aortic hematopoietic clusters that express Runx1 and Kit. However, mutant cells fail to mature into blood lineage cells both in vivo and in vitro, and instead undergo apoptosis. Gene expression profiling of the E10.5 mutant endothelium revealed that Chd1 is required for the activation of a transcriptional sub-program associated with hematopoiesis and cellular growth. We found that emerging hematopoietic progenitors

have an elevated transcriptional output relative to structural endothelium, and this elevation is suppressed in *Chd1* mutants. Finally, hematopoietic-specific deletion of *Chd1* using *Vav-Cre* yields no apparent defects during development or adulthood. These results indicate that Chd1 promotes an elevated transcriptional output that is essential during a specific developmental window in the transition of endothelial cells to definitive blood progenitors.

Table of Contents

List of tables

List of figures

Chapter 1

Parallel gateways to pluripotency:

open chromatin in stem cells and development

Abstract

Open chromatin is a hallmark of pluripotent stem cells, but the underlying molecular mechanisms are only beginning to be unraveled. In this review we highlight recent studies that employ embryonic stem cells and induced pluripotent stem cells to investigate the regulation of open chromatin and its role in the maintenance and acquisition of pluripotency *in vitro*. We suggest that findings from *in vitro* studies using pluripotent stem cells are predictive of *in vivo* processes of epigenetic regulation of pluripotency, specifically in the development of the zygote and primordial germ cells. The combination of *in vitro* and *in vivo* approaches is expected to provide a comprehensive understanding of the epigenetic regulation of pluripotency and reprogramming.

Introduction

Pluripotent stem cells have a limitless capacity for self-renewal and the unique potential to differentiate into all cell types. With the advent of techniques to reprogram somatic cells into pluripotent stem cells, there is an increased interest in understanding the mechanisms that underlie the maintenance and acquisition of pluripotency. Such understanding may provide important new insights into the regulation of embryonic development, and contribute to the generation of patient-specific pluripotent stem cells for disease modeling and cell replacement therapies.

While transcriptional differences between somatic cells and pluripotent stem cells are well established, there is increasing evidence supporting the critical role that chromatin accessibility plays in pluripotent stem cells. In this review, we highlight recent advancements in our understanding of how open chromatin regulates the maintenance and acquisition of pluripotency. We first describe epigenetic remodelers that regulate open chromatin *in vitro* in pluripotent embryonic stem (ES) cells and reprogrammed induced pluripotent stem (iPS) cells. The large number of ES and iPS cells that can be grown *in vitro* has facilitated the dissection of epigenetic regulation of pluripotency in these cells. We then discuss the potential significance of these recent findings *in vivo*. We propose that epigenetic mechanisms used to maintain and acquire pluripotency *in vitro* operate *in vivo* in the acquisition of totipotency in the nascent zygote and maintenance of pluripotency in germ cells. The integration of studies *in vitro* and *in vivo* should thus significantly augment our global understanding of the epigenetic regulation of pluripotency and embryonic development.

ES cell cultures may reflect distinct *in vivo* epigenetic states

ES cells are pluripotent stem cells derived from the inner cell mass of the blastocyst, prior to implantation, and they serve as an excellent *in vitro* model for probing the molecular mechanisms that govern cell fate decisions during early development. Recent data indicate that ES cells are not a homogeneous cell population as previously thought, but rather oscillate between different cell states that may have parallels *in vivo* (Chambers et al., 2007; Cui et al., 2004; Furusawa et al., 2004; Hayashi et al., 2008; Toyooka et al., 2008). Mouse ES cell cultures contain significant heterogeneity: the core pluripotency gene Nanog (Chambers et al., 2007) and stem-cell markers Rex1 (Toyooka et al., 2008), Pecam1 (Cui et al., 2004), SSEA1 (Cui et al., 2004; Furusawa et al., 2004) and Stella (Hayashi et al., 2008) have all been shown to exhibit a heterogeneous expression pattern, where ES cells are in flux between high and low expression of these genes. The variable phenotype correlates with *in vivo* expression patterns and appears to represent two distinct yet reversible embryonic stages: one that reflects an inner cell mass-like state, and another that is closer to an epiblast-like state (Furusawa et al., 2004; Hayashi et al., 2008; Toyooka et al., 2008).

Strikingly, populations enriched for pluripotency markers SSEA1 or Stella are able to restore the original ratio of mixed populations (Cui et al., 2004; Hayashi et al., 2008). Stella expression levels correlate with the presence of activating histone marks H3K9ac and H3K4me3 at the Stella gene locus. Interestingly, the Stella+ sub-population is lost when ES cells are cultured in the absence of embryonic fibroblast feeder cells, and addition of the histone deacetylase inhibitor trichostatin A, which promotes active

transcription, restores Stella expression in feeder-free conditions (Hayashi et al., 2008). Taken together, the data available suggest that extracellular signaling within ES cell cultures, and potentially *in vivo*, regulates gene expression and differentiation through epigenetic changes. Further evidence comes from a recent study demonstrating that ES cell-like cultures containing a Stella+ sub-population can be derived directly from epiblast tissue or epiblast stem cells after prolonged culture with LIF-fetal calf serum on mouse embryonic fibroblast feeders (Bao et al., 2009). This transformation is accompanied by DNA demethylation at the Stella and Rex gene loci, further supporting an epigenetic switch between the epiblast and inner cell mass-like states.

Direct evidence of epigenetic regulation of cell-fate comes from studies of two closely related DNA-binding transcriptional regulators that are involved in higher-order chromatin organization, Satb1 (Cai et al., 2006) and Satb2 (Dobreva et al., 2006). The two Satb proteins appear to regulate ES cell self-renewal in an antagonistic manner: while both factors can bind to the Nanog promoter, Satb1 acts to repress Nanog transcription, and Satb2 appears to activate it. Therefore, the balance of Satb1 and Satb2 may underlie the heterogeneity of Nanog expression in ES cells (Savarese et al., 2009). However, it remains to be seen if extracellular signals lie upstream of these factors. It will be interesting in future studies to determine how LIF and other extracellular signals interact with epigenetic regulators to control pluripotency in ES cells and during development.

New epigenetic regulators of pluripotency

Pluripotent stem cells maintain a globally open chromatin state (Efroni et al., 2008; Meshorer et al., 2006), possibly so that genes are readily available for activation during tissue specification (Efroni et al., 2008). ES cells have low levels of dense, compacted chromatin (heterochromatin) and the ES cell genome is transcriptionally hyperactive, with widespread transcription in both coding and non-coding regions, including sporadic low-level expression of tissue specific genes (Carter et al., 2005; Efroni et al., 2008). In addition, a recent study showed that the distribution of repressive marks H3K9me3 and H3K27me3 are significantly expanded in somatic cells relative to pluripotent stem cells (Hawkins et al., 2010). In agreement with these observations, chromatin remodeling factors are over-represented in the ES cell transcriptome, and RNAi knockdown of several chromatin remodelers like Chd1 and Brg1 has been shown to severely impact ES cell proliferation and differentiation potential (Efroni et al., 2008; Gaspar-Maia et al., 2009).

Chd1 is a chromatin remodeler associated with active transcription that contains a helicase domain, a DNA-binding domain and a pair of chromodomains that binds selectively to the euchromatin mark H3K4me2/3 (Gaspar-Maia et al., 2009; Sims et al., 2005; Stokes et al., 1996) (reviewed in (Persson and Ekwall, 2010)). Chd1 is required to maintain the open chromatin state of pluripotent mouse ES cells (Figure 1). Chd1-deficient ES cells show an increased number of heterochromatin foci and a pluripotency defect characterized by a high propensity for neural differentiation and an absence of primitive endoderm (Gaspar-Maia et al., 2009). The molecular mechanism by which

Chd1 regulates open chromatin of ES cells remains unknown. Chromatin immunoprecipitation using promoter tiling arrays shows that Chd1 binding overlaps with markers of transcription, including RNAPolII and H3K4me3 (Gaspar-Maia et al., 2009). Interestingly, this distribution at gene promoters is similar to that of histone variant H3.3 (Goldberg et al., 2010). H3.3 is correlated with sites of active transcription in many species (Chow et al., 2005; Mito et al., 2005; Schwartz and Ahmad, 2005) and appears to maintain open chromatin by inhibiting histone H1 binding to the nucleosome (Braunschweig et al., 2009) (reviewed in (Elsaesser et al., 2010)). The incorporation of H3.3 in ES cells is complex and includes the promoters of active and repressed genes, gene bodies only in active genes, transcriptional factor binding sites and telomeres (Goldberg et al., 2010). Evidence from *Drosophila* suggests that Chd1 is required for H3.3 incorporation into chromatin (see below) (Konev et al., 2007). It will therefore be of interest to characterize the genomic distribution of Chd1 binding in ES cells beyond gene promoters, determine which aspects of H3.3 incorporation, if any, are dependent on Chd1, and test whether H3.3 mediate the pluripotency defects in Chd1-deficient ES cells.

The BAF (Brg/Brahma-associated factors) complex is a chromatin remodeler of the SWI/SNF family that has been shown to regulate pluripotency (Ho et al., 2009b). ES cells express a distinctive BAF complex (esBAF) defined by the presence of Brg1 (Brahma-related gene 1), BAF155, and BAF60A, and the absence of Brahma, BAF170, and BAF60C. Using genome-wide ChIP-seq technology, Brg1 was shown to co-localize extensively with the pluripotency transcription factors Oct4, Sox2, and Nanog, thereby

suggesting a pluripotency-specific role for esBAF (Ho et al., 2009a). In addition, Brg1 does not share many targets with the polycomb repressive complex PRC2, suggesting that esBAF is an activator of transcription.

Polycomb repressive complexes (PRCs) coordinate the transcriptional repression of lineage-specific developmental genes in ES cells in multiple ways, including mediating H3K27 di-/tri-methylations and H2A ubiquitination (Boyer et al., 2006; Ku et al., 2008; Mikkelsen et al., 2007). Disruption of either PRC1 or PRC2 results in early embryonic lethality *in vivo* (O'Carroll et al., 2001; Voncken et al., 2003; Wang et al., 2002). This observation is mirrored *in vitro* by the propensity of PRC1- or PRC2-deficient ES cells to differentiate (Boyer et al., 2006; Leeb et al., 2010). Cell survival is greatly reduced upon initiation of differentiation in PRC-deficient ES cells, possibly due to activation of endogenous retroviruses (Leeb et al., 2010). Novel components of the PRC2 complex have recently been shown to be enriched in undifferentiated ES cells: Jarid2 was identified as a regulatory component that modulates PRC2 localization and activity (Peng et al., 2009; Shen et al., 2009), and Pcl2 was described as another component required for proper regulation of both pluripotency and lineage-specific genes in ES cells (Walker et al., 2010).

Finally, DNA methylation is another epigenetic mechanism by which ES cells may regulate gene expression. Recent studies challenge the classical view that ES cells have reduced global DNA methylation, but rather reveal that they use ES cell-specific non-CpG methylation in addition to the canonical CpG methylation (Laurent et al., 2010; Lister et al., 2009). While DNA methylation is generally associated with transcriptional

silencing, the functional significance of this alternative type of DNA methylation in ES cells remains to be determined. It should also be noted that a marker of active transcription, H3K36me3, is highly correlated with the presence of DNA methylation within gene bodies, suggesting a role for DNA methylation beyond transcriptional repression (Hawkins et al., 2010; Jones, 1999). Future investigations will be necessary to explore the functional significance of this alternative regulatory node.

In sum, recent findings indicate that the open, accessible chromatin state of ES cells is actively maintained by chromatin remodelers such as Chd1, and that PRCs and DNA methylation are involved in repression of developmental genes until differentiation is triggered. Therefore, a complex, dynamic balance is at play in the epigenetic regulation of ES cell pluripotency. How this balance may be reestablished during reprogramming of somatic cells to pluripotency is the focus of the next section.

Reacquiring pluripotency *in vitro*: epigenetics is key

Cellular reprogramming by the ectopic expression of defined transcription factors offers a reliable, albeit inefficient, method of obtaining iPS cells from somatic cells (Takahashi and Yamanaka, 2006). Although detailed analyses comparing mouse and human ES and iPS cells have uncovered subtle differences in gene expression patterns (Chin et al., 2009), iPS cells have consistently been found to re-activate pluripotency-related genes as well as re-establish an ES cell-like open chromatin state via global DNA demethylation and H3K4 and H3K27 methylation changes (Chin et al., 2009;

Maherali et al., 2007; Mikkelsen et al., 2008). Therefore, it is expected that global chromatin opening and DNA demethylation will be important components of reprogramming (Figure 1).

In order to gain insight into the epigenetic changes that may underlie reprogramming, several groups have compared stable partially reprogrammed cell lines, which have not turned on the endogenous Oct4 gene, to true iPS cells that have activated Oct4 (Meissner et al., 2007; Mikkelsen et al., 2008; Sridharan et al., 2009). These partially reprogrammed cells exhibit DNA hypermethylation and a failure to remethylate H3K4 relative to ES and true iPS cells (Mikkelsen et al., 2008), supporting the notion that proper epigenetic remodeling may be required for successful reprogramming to pluripotency. Direct manipulation of the chromatin of these partially reprogrammed cells and of somatic cells during reprogramming have proved to be effective at enhancing reprogramming efficiency. DNA methyltransferase inhibitor 5-azacytidine (5-azaC) induces partially reprogrammed cells to undergo a rapid and stable transition to a fully reprogrammed state (Mikkelsen et al., 2008), while 5-azaC and histone deacetylase inhibitors like valproic acid increase the efficiency of iPS cell generation up to 40-fold (Huangfu et al., 2008). These observations parallel earlier ones made using somatic cell nuclear transfer (SCNT), which established DNA demethylation of somatic cell nuclei as a necessary step to successful reprogramming in mouse and *Xenopus* (Blelloch et al., 2006; Simonsson and Gurdon, 2004).

In addition, targeted downregulation by RNAi has enabled the identification of specific molecular complexes involved in the reprogramming process. Downregulation

of Chd1, a regulator of open chromatin and pluripotency of ES cells (see above), strongly inhibits generation of iPS cells (Gaspar-Maia et al., 2009). It will be of interest to determine whether H3.3 incorporation or other functions associated with Chd1 underlie its role in reprogramming. Recently, activation-induced cytidine deaminase (AID), which is involved in DNA demethylation (Rai et al., 2008), has been implicated in reprogramming. Knockdown of AID during nuclear reprogramming by somatic cell fusion with ES cells leads to a failure to reactivate Oct4 and Nanog, possibly due to defective DNA demethylation at their promoters (Bhutani et al., 2010). Future work using RNAi screens will likely elucidate other molecular complexes involved in reprogramming towards pluripotency *in vitro*.

While studies of the epigenetic regulation of iPS cell generation are expected to have broad application in regenerative medicine, they may in addition reveal potential molecular parallels between experimental reprogramming *in vitro* in iPS cells and physiological reprogramming *in vivo* (Ramalho-Santos, 2009). In the next sections we describe some of these potential parallels, focusing on recent insights into epigenetic reprogramming in the zygote and mid-gestation germ cells (Figure 1).

Epigenetic reprogramming towards totipotency in the zygote

The zygote marks the starting point of development, and represents the reacquisition of totipotency from fusion of two highly differentiated gametes. The two parental genomes in the zygote have highly asymmetric chromatin organization

(Puschendorf et al., 2008; van der Heijden et al., 2005). Most histones are stripped from the paternal genome during spermatogenesis and replaced with highly basic protamines that allow for a very tight compaction of DNA (Balhorn, 2007; Ward, 1991; Wykes and Krawetz, 2003). A restricted set of nucleosomes is retained in about 4% of the genome, preferentially at developmental genes (Hammoud et al., 2009). These histones appear to be enriched in modifications like H3K27me3 and H3K4me3 in patterns that overlap significantly with those in ES cells. It thus appears that sperm DNA, while densely packed with protamines, may also transmit epigenetic marks important for early development (Hammoud et al., 2009).

Shortly after fertilization, H3.3 is preferentially incorporated into the male pronucleus (Torres-Padilla et al., 2006; van der Heijden et al., 2005), presumably by maternal stores of chromatin factors that complement the transcriptionally silent zygote (Latham et al., 1992; Levey et al., 1978; Schultz, 2002). Although these factors have not been characterized in the mammalian zygote, maternal Chd1 has been shown to be required for incorporation of H3.3 into the male pronucleus in the *Drosophila* embryo (Konev et al., 2007). *Drosophila* embryos derived from Chd1-null mothers exhibit a loss of the paternal genome and the resulting haploid embryos arrest before hatching. Functional studies of Chd1 in mouse should reveal whether its role in H3.3 incorporation in the male pronucleus is conserved, and if so, what is the significance of this process for mammalian development (Figure 1).

Another important epigenetic asymmetry between the parental genomes is that paternal (but not maternal) DNA is actively demethylated immediately following

fertilization (Barton et al., 2001; Oswald et al., 2000). No DNA demethylase has been described despite extensive efforts (Ooi and Bestor, 2008). With the aid of a live cell imaging reporter system, a recent RNAi screen implicated the transcription elongator complex in paternal DNA demethylation (Okada et al., 2010). The molecular mechanism behind elongator-mediated DNA demethylation needs to be further explored. In addition, it will be important to determine whether this represents a unique DNA demethylation mechanism, or whether AID is involved. Finally, the relationship between H3.3 incorporation and DNA demethylation, both of which occur prior to the first cell division, remains to be explored.

Epigenetic reprogramming in primordial germ cells

Another context where extensive chromatin remodeling occurs *in vivo* that may have parallels with reprogramming *in vitro* is in primordial germ cells (PGCs). PGCs are specified by inductive signals around the time of gastrulation and represent the only lineage from the epiblast that actively represses the somatic cell fate in order to form oocytes and sperm later in development (reviewed in (Sasaki and Matsui, 2008)). PGCs are also the only embryonic cells post-gastrulation that can still give rise to pluripotent stem cells when cultured *in vitro* (Resnick et al., 1992). These observations, coupled with the large number of regulators of ES cell pluripotency that are expressed in PGCs (Grskovic et al., 2007), suggest that some of same molecular mechanisms that maintain pluripotency *in vitro* may operate in PGCs.

Several recent studies (Hajkova et al., 2008; Seki et al., 2007; Yabuta et al., 2006) paint an intricate picture of the dynamic epigenetic reprogramming that takes place *in vivo* during PGC maturation. PGCs experience a large-scale loss of DNA methylation (Hajkova et al., 2002; Lee et al., 2002; Popp et al., 2010) and many histone marks, including H3K9Ac, H3K9me3 and H3K27me3, around E11.5. Concurrently, linker histone H1 staining is lost and DAPI-stained chromatin becomes noticeably 'loosened'. Subsequently by E12.5, the transient loosening of the chromatin is reversed with the return of brightly stained DAPI foci, histone H1, H3K9me3, H3K27me3 and pericentromeric heterochromatin marks (Hajkova et al., 2008).

It is possible that the rapid chromatin opening in E11.5 PGCs results from a large-scale incorporation of H3.3. In support of this hypothesis, the histone chaperone HIRA, which is essential for delivering H3.3 to active and repressed genes (Ahmad and Henikoff, 2002; Goldberg et al., 2010), is enriched in the nucleus of E11.5 PGCs (Goldberg et al., 2010; Hajkova et al., 2008). Chd1, which directly facilitates H3.3 deposition (Konev et al., 2007), is highly expressed in E11.5 PGCs (Grskovic et al., 2007). Finally, H3.3 is essential for chromatin remodeling in the *Drosophila* germline, with both male and female flies mutant for H3.3 being sterile (Hödl and Basler, 2009; Sakai et al., 2009). Altogether, it is tempting to speculate that maintenance of germline pluripotency, from flies to mice, requires the deposition of H3.3 by Chd1. It will therefore be of great interest to determine the function of Chd1, HIRA and H3.3 during mammalian PGC development (Figure 1).

The functional significance of this large-scale chromatin remodeling in PGCs remains unclear, but it may limit the transmission of epigenetic information across generations. It may not be a coincidence that, as in the case of the zygote, extensive chromatin remodeling in PGCs coincides with large-scale DNA demethylation (Hajkova et al., 2002). Careful observations suggest that DNA demethylation may precede chromatin remodeling in PGCs (Hajkova et al., 2008), but this remains to be demonstrated functionally. Intriguingly, AID was recently shown to be essential for efficient DNA demethylation in PGCs (Popp et al., 2010), highlighting another potential parallel between reprogramming in PGCs and *in vitro*.

Perspectives and future directions

Increasing evidence supports the notion that an open, decondensed chromatin state plays a vital role in the regulation of pluripotency in stem cells *in vitro* and during critical events of mammalian embryogenesis, including zygote and PGC development. The ease with which ES and iPS cells can be obtained in large numbers allows the application of unbiased genome-wide approaches such as ChIP-Seq and RNAi screens. The integration of data from these approaches should shed light on the epigenetic architecture of the pluripotent stem cell state, and how it is reconfigured during differentiation. The process of reprogramming to iPS cells remains largely a black box, and future studies are likely to reveal the epigenetic steps undertaken by somatic cells on the way to the open pluripotent chromatin state. The limited numbers of zygotes and

PGCs and their rapidly changing transcriptional and epigenetic states during embryonic development pose significant technical hurdles to genome-wide analyses. Nevertheless, recent advancements have made genome-wide studies of chromatin states feasible for limited numbers of primary cells, and we expect that novel insights will be gained from applying these methods to pluripotent cells *in vivo*. In addition, candidate gene approaches that determine the *in vivo* roles of regulators of the open chromatin state of pluripotent stem cells, such as Chd1, may reveal common themes in the regulation of open chromatin. Research in the years ahead will likely reveal fascinating insights into the epigenetic regulation of pluripotency *in vitro* and its significance *in vivo*.

Figure 1. Potential parallels in epigenetic regulation of pluripotency in stem cells *in vitro* and the germline *in vivo*.

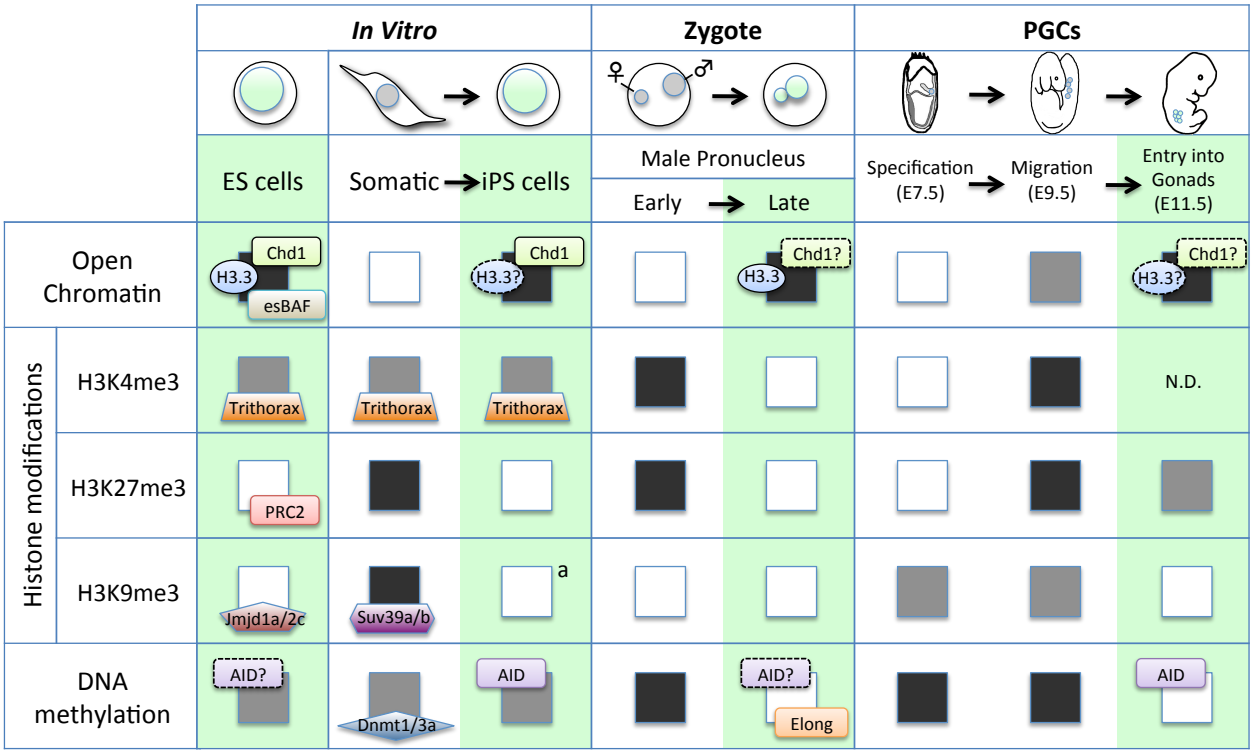

Footnotes:

a iPS cells have a significant expansion of H3K9me3 into genes compared to ES cells.

N.D. Not determined.

Figure 1. Potential parallels in epigenetic regulation of pluripotency in stem cells *in vitro* and the germline *in vivo*.

ES and iPS cells are useful *in vitro* models to study the regulation of open chromatin and associated epigenetic marks in pluripotent cells. Several epigenetic regulators have been shown to be important for the establishment and maintenance of the open chromatin state of pluripotent stem cells, although the picture is far from complete. Much less is known about the epigenetic regulators that operate *in vivo* in epigenetic reprogramming in the early zygote and PGCs. Note that the column "zygote" refers to chromatin decondensation of the male pronucleus after fertilization. Recent evidence suggests that Chd1 and AID are essential chromatin regulators of pluripotency both *in vitro* and *in vivo*. Future studies may reveal the potential molecular parallels, as well as the differences, in epigenetic regulation between the various cell types depicted. Shaded columns represent cell types and states associated with open chromatin. For simplicity, several chromatin factors known to have roles in each specific cell type are not shown. See text in Chapter 1 for details.

Chapter 2

Chd1 regulates the emergence of definitive hematopoietic stem and progenitor cells

Abstract

Lineage specification during development involves reprogramming of transcriptional states, but little is known about how this is regulated in vivo. The chromatin remodeler Chd1 promotes an elevated transcriptional output in mouse embryonic stem cells. Here we report that endothelial-specific deletion of *Chd1* leads to loss of definitive hematopoietic progenitors, anemia and lethality by E15.5. Mutant embryos contain normal numbers of E10.5 intra-aortic hematopoietic clusters that express Runx1 and Kit, but these clusters undergo apoptosis and fail to mature into blood lineages in vivo and in vitro. Hematopoietic progenitors emerging from the aorta have an elevated transcriptional output relative to structural endothelium, and this elevation is Chd1-dependent. In contrast, hematopoietic-specific deletion of *Chd1* using *Vav-Cre* has no apparent phenotype. Our results reveal a new paradigm of regulation of a developmental transition by elevation of global transcriptional output that is critical for hemogenesis and may play roles in other contexts.

Introduction

Hematopoiesis occurs in successive waves and in distinct regions of the embryo during vertebrate development (Cumano and Godin, 2007; Dzierzak and Speck, 2008). Primitive hematopoiesis begins in the extra-embryonic yolk sac at embryonic day (E) 7.0 and consists primarily of primitive erythroid cells (Palis et al., 1999). These progenitors begin to circulate upon the onset of cardiovascular function, migrating to the developing fetal liver (FL) to support early embryonic development via primitive erythropoiesis (Baron et al., 2012). Definitive hematopoietic stem cells (HSCs), which have the ability to self-renew and reconstitute all blood lineages in adult recipients, arise from hemogenic endothelium at various vascular sites beginning around E10 (Chen et al., 2009; de Bruijn et al., 2002; Zovein et al., 2008). These sites include the aorta-gonad-mesonephros (AGM), umbilical and vitelline arteries, and the placenta, among others (Swiers et al., 2013; Zape and Zovein, 2011). The endothelial-to-hematopoietic transition (EHT) is best characterized in the AGM, where clusters of hematopoietic stem and progenitor cells (HSPCs) have been observed to emerge from the ventral wall of the dorsal aorta (Bertrand et al., 2010; Boisset et al., 2010; Kissa and Herbomel, 2010). The molecular regulation of this remarkable developmental transition is poorly understood, but would likely involve a resetting of the transcriptional program of the endothelium to that of hematopoietic progenitors. In agreement with this notion, the transcription factors *Runx1* (Chen et al., 2009) and *Gata2* (de Pater et al., 2013) have been shown to be critical for this transition. It remains unclear what gene expression programs these

transcription factors regulate, and whether chromatin regulators also play a role in this transition.

Chromodomain helicase DNA-binding protein 1 (Chd1) is an ATP-dependent chromatin-remodeling enzyme that binds specifically to di- and tri-methylated H3K4 (Flanagan et al., 2005) and is associated with actively transcribed genes. Chd1 has been linked to various transcription-related processes, including regulation of nucleosome positioning at the 5' end of transcribed genes (Gkikopoulos et al., 2011; Skene et al., 2014), suppression of cryptic transcription (Quan and Hartzog, 2010; Smolle et al., 2012), transcriptional elongation (Lin et al., 2011; Quan and Hartzog, 2010; Simic et al., 2003), and coupling of transcription with splicing (Sims et al., 2007). We have previously described *Chd1* as a gene up-regulated in multiple mouse stem and progenitor cell types (Grskovic et al., 2007; Ramalho-Santos et al., 2002). We subsequently showed that Chd1 binding correlates with H3K4me3 and RNA Polymerase II binding at transcriptional start sites in mouse embryonic stem (ES) cells, and that Chd1 regulates ES cell self-renewal and reprogramming efficiency in induced Pluripotent Stem (iPS) cells (Gaspar-Maia et al., 2009). Moreover, we recently found that Chd1 promotes an elevated transcriptional output by RNA Polymerases I and II, and is required for the survival and growth of the E5.5 epiblast (Guzman-Ayala et al., 2015).

In this study, we investigated the role of Chd1 in the endothelial-to-hematopoietic transition. We report that endothelial-specific deletion of a conditional *Chd1* allele using *Tie2-Cre* results in a block in definitive hematopoiesis. Lack of Chd1 in endothelial cells

results in embryonic lethality by E15.5 due to a complete failure of definitive erythropoiesis, and subsequent anemia that is incompatible with development to term. We further show that, while intra-aortic hematopoietic clusters develop in the mutant AGM at E10.5 at a normal frequency and express intermediate markers of differentiation, these clusters do not mature into blood lineage cells in vitro or in vivo. The transcriptome of the mutant endothelium is largely unchanged but lacks activation of a set of genes highly enriched for hematopoietic and growth functions. Interestingly, we found that emerging hematopoietic progenitors undergo an elevation in global transcriptional output that is dependent on Chd1. On the other hand, deletion of *Chd1* specifically in hematopoietic cells using *Vav-Cre* has no phenotype, indicating that *Chd1* is not required for hematopoietic survival or function after the endothelial-to-hematopoietic transition. Taken together, these results define a narrow but critical window in which a Chd1-driven elevation in transcriptional output is essential for the developmental transition from endothelium to definitive hematopoiesis in the mouse embryo.

Results

Endothelial-specific deletion of Chd1 results in embryonic lethality

Given the difficulty in using commercial antibodies to detect Chd1 by immunostaining, we assessed Chd1 expression using a mouse line carrying a β-galactosidase reporter knocked into the endogenous *Chd1* locus (*Chd1*^{LacZ}) (Guzman-Ayala et al., 2015). These results revealed that *Chd1* is broadly though not uniformly expressed at mid-gestation (Figure S1A). The expression of *Chd1* is higher in mesodermal tissues, with low to undetectable expression in the neural tube and intestinal epithelium. In particular, we noticed that *Chd1* is expressed in endothelial cells throughout the embryo, including the lung vasculature, the intramedullary blood vessels of the spinal cord, and the ductus venosus in the FL (Figure S1B). We therefore sought to assess the potential role of *Chd1* in the endothelium and its derivatives.

Chd1$^{-/-}$ embryos arrest at E5.5-6.5 due to a defect in epiblast survival and proliferation (Guzman-Ayala et al., 2015), necessitating the use of conditional gene deletion strategy to assess the roles of *Chd1* post-gastrulation. Mice carrying a floxed allele of *Chd1* (*Chd1*$^{flox/flox}$) (Guzman-Ayala et al., 2015) were crossed to a transgenic mouse line that expresses Cre recombinase under the control of the *Tie2* promoter (*Tie2-Cre*; Figure S2A), so as to delete *Chd1* specifically in the endothelium (Braren et al., 2006). To verify recombination efficiency of *Tie2-Cre*, we included in our breeding scheme a Cre reporter allele, *Ai14* (Madisen et al., 2010). This reporter consists of a red fluorescent protein tdTomato (tdT) under a ubiquitous CAG promoter, inserted in the

Rosa26 locus, and preceded by a loxP-flanked STOP cassette. We achieved a high percentage of recombination within the endothelium population ($CD31^+$) with *Tie2-Cre*, with 76% of E9.5 (n=28) and 84% of E10.5 (n=27) $CD31^+$ cells expressing tdTomato (Figure S2B). Mutant embryos carry the *Tie2-Cre; Chd1*$^{flox/-}$ genotype, and the loss of *Chd1* in these embryos was validated using qRT-PCR and microarrays (Figures S2C, S2D and see below). As controls, we use *Tie2-Cre; Chd1*$^{flox/+}$ embryos ("CreHet"), in which Cre induces a heterozygous state for *Chd1* in the endothelium. There is no significant difference in recombination efficiency between CreHet control and mutant embryos (Figure S2B). Embryos at E11.5 display extensive recombination and red fluorescence in the endothelium throughout the embryo and in the yolk sac as expected (Figures S2E and S2F).

Chd1 mutant pups cannot be recovered at birth, indicating that Chd1 plays an essential role in the endothelium (n=123 pups from 23 litters, $p<0.0001$, χ^2 test) (Table 1). CD31 immunostaining of E10.5 yolk sac reveals similar branching of blood vessels between mutants and controls (Figure S2F), suggesting that early endothelial patterning is not affected by the loss of Chd1. In addition, mutants at E13.5 have normal beating hearts (data not shown) and no discernible defects in the development of the four chambers (Figure S3A), indicating that heart development is unaffected by endothelial *Chd1* ablation. Mutant embryos are morphologically distinguishable at E13.5 from littermate controls, appearing paler and exhibiting hemorrhage and edema (Figure 2A). By E15.5, most mutant embryos are resorbed (n=60 embryos from 9 litters, $p=0.021$, χ^2 test). Hemorrhage and edema are characteristic of lymphatic defects, and we verified

that the prominent bilateral hemorrhage around the forelimbs in E13.5 mutant embryos is a result of blood accumulation in dilated jugular lymph sacs and other lymphatic vessels (Figure S4). Unlike endothelial *Chd1* mutants, embryos with mutations that disrupt the blood-lymphatic separation survive to the perinatal period (Cheng et al., 1995; Saleque et al., 2002; Turner et al., 1995; Uhrin et al., 2010; Wang et al., 2000). Moreover, mutations in regulators of the EHT, such as *Runx1* (Srinivasan et al., 2007), *Gata2* (Lim et al., 2012) and β-catenin (Ruiz-Herguido et al., 2012), display lymphatic phenotypes similar to those seen in *Chd1* mutants. This is likely due to a requirement of intact platelet function for proper separation of blood and lymphatic circulatory systems (Uhrin et al., 2010). Therefore, we conclude that the lymphatic system defects are not the primary cause of lethality of *Chd1* mutants, and may be secondary to a role in hemogenesis.

Endothelial *Chd1* mutants die from severe anemia

Mutant embryos at E11.5 show no signs of the edema and hemorrhage typical of lymphatic defects, but already tend to be paler than controls, particularly in the yolk sac (Figure S3B). As the FL is a major erythropoietic organ from E10 until shortly before birth (Baron et al., 2012), we isolated FLs from E13.5 embryos. Mutant E13.5 FLs are significantly paler and smaller compared to those of littermate controls (Figure 2B). The cellularity of mutant FLs is reduced to about 18% of the level of CreHets [average of 1.6 $x10^6$ cells in mutants (n=8), relative to an average of 8.8 $x10^6$ cells in CreHets (n=9),

p<0.0001] (Figure 2C). We used flow cytometry to analyze E13.5 FLs for Kit, a marker for definitive erythroid progenitors at this stage (Fraser et al., 2007; Isern et al., 2011). While almost half of CreHet FL cells are Kit^+ (48.8%, n=8), mutants show a severe reduction of Kit^+ progenitors where only 20.0% of FL cells are Kit^+ (n=18, p<0.0001) (Figures 2D and 2E). FLs harvested from E11.5 embryos have a similar reduction in Kit^+ cells, indicating that blood progenitors are reduced as early as E11.5 (Figures 2D and 2E).

To functionally test for FL erythropoietic activity, we evaluated E13.5 FL using colony-forming unit-erythroid (CFU-E) assays by seeding equal numbers of FL cells into methylcellulose containing only erythropoietin. CFU-Es are reduced in mutants to 28.5% of the level in CreHets (n=9 mutants vs n=14 CreHets, p<0.0001, Figure 3A). This decrease prompted us to evaluate immature erythroid progenitors (burst-forming unit-erythroid, BFU-E) using additional growth-promoting cytokines (IL3, IL6 and SCF/Kitl). BFU-Es are greatly reduced in mutants, to 32.1% of the level in CreHets (n=12 mutants vs n=12 CreHets, p<0.0001, Figure 3B). In contrast, we did not observe significant differences between mutants and CreHets in the number of multi-lineage colonies (CFU-GM and CFU-GEMM) (Figures 3C and 3D). These results indicate that *Chd1* mutant FLs are not only greatly reduced in total cell number, but are also depleted of erythroid progenitor cells when equal numbers of cells are assessed.

To determine the cause of the reduced erythroid population, we examined the cell cycle profile of E13.5 FL cells by the incorporation of 5-ethynyl-2'-deoxyuridine (EdU). While almost half of the cells in control FLs are in S phase (47.8%, n=11), only

18.0% of the cells in mutant FLs (n=3) are in S phase, indicating a reduced proliferation capacity in the mutants (Figures 3E and 3F). To determine if the remaining erythrocytes present in the E13.5 mutant FL are predominantly of the primitive or definitive lineage, we conducted qRT-PCR for globin genes that are differentially expressed between the two lineages (Kingsley et al., 2006). We found that mutant Ter119^{+} erythrocytes had higher levels of primitive globin expression (ζ-globin, εγ-globin and βH1-globin) and reduced expression of β1-globin, which is associated with definitive erythrocytes (Figure 3G). This result indicates that mutants have a higher ratio of primitive to definitive Ter119^{+} erythrocytes in the FL compared to CreHet controls. Taken together, we conclude that endothelial *Chd1* mutants experience anemia due to a failure in definitive erythropoiesis.

Definitive hematopoiesis is impaired in *Chd1* mutants

The strong reductions in total FL cellularity and erythropoiesis in the mutants led us to explore potential defects in hematopoietic progenitors. We found that the percentage of Ter119^{-} Kit^{+} Sca1^{+} hematopoietic stem and progenitor cells (HSPCs) is reduced by 3-fold in E13.5 mutant FLs, from 3.0% in CreHets (n=8) to 0.9% in mutants (n=18, $p<0.0001$) (Figures 4A and 4B). Importantly, this reduction in HSPCs is present as early as E11.5, where control FLs had 1.7% Ter119^{-} Kit^{+} Sca1^{+} HSPCs (n=10) compared to 0.4% in mutants (n=15, $p<0.0001$) (Figures 4A and 4B). Thus, HSPCs are reduced in endothelial *Chd1* mutants, both in absolute number and relative frequency.

Whereas the FL is the site of HSPC expansion and differentiation, the endothelium of the AGM at E10.5 is a source of definitive hematopoietic progenitors via an endothelial-to-hematopoietic transition (de Bruijn et al., 2000). To determine if the depletion of HSPCs in the FL can be traced back to defective AGM hematopoiesis, we assessed the emergence of intra-aortic hematopoietic clusters in E10.5 AGMs. Confocal imaging of mutant AGMs revealed the presence of intra-aortic clusters that express known HSPC markers Runx1 (n=4) and Kit (n=2) (Figures 5A and S5). Mutants also had no significant difference in the number of hematopoietic clusters compared to CreHets (Figure 5B, n=6). These data suggest that *Chd1*-deficient hemogenic endothelium is capable of forming hematopoietic clusters in the AGM. However, hematopoietic clusters in mutant AGMs show signs of apoptosis, as indicated by staining for cleaved caspase-3, which was not detected in any of the clusters examined in CreHet AGMs (Figure 5C). To determine if the apoptosis seen in mutant hematopoietic clusters could affect the maturation of hemogenic endothelium into HSPCs, we examined E11.5 AGM $CD31^+$ endothelial cells for hemogenic activity. Flow analyses revealed that the proportion of Kit^+ $CD45^-$ cells (early cluster cell markers) within the $CD31^+$ endothelial population in the AGM at E11.5 is similar between mutants and CreHet controls. However, there is a significant reduction in Kit^+ $CD45^+$ cells (HSPC markers) in the mutants compared to CreHet controls (Figures 5D and 5E), suggesting a potential failure in the maturation to $CD45^+$ HSPCs in *Chd1* endothelial mutants.

To functionally assess the EHT potential in the mutants, we evaluated the ability of E10.5 AGMs to differentiate into myeloid and lymphoid cells in vitro. Methylcellulose

colony assays revealed that mutant AGMs yield an average of 24.9 colonies (n=8) vs 142.7 colonies in CreHets (n=6) (Figure 5F), indicating that mutants have more than 5-fold reduction in myeloid potential than CreHets. To test for lymphoid lineage differentiation potential, we cultured E10.5 AGMs on OP9-DL1 stromal cells, which have previously been shown to support T lymphocyte differentiation in vitro (Schmitt et al., 2004). While AGMs taken from CreHet embryos can differentiate into $CD45^+$ $TCR\beta^+$ T lymphocytes in vitro, mutant AGMs are strongly impaired in the generation of $CD45^+$ blood cells in this culture system (Figure 5G), in agreement with data in vivo (Figures 5D and 5E), and do not show evidence of TCRβ expression (Figure 5H). Taken together, these results indicate that the endothelial-to-hematopoietic transition is initiated in the mutant AGM, but the maturation into HSPCs is defective, resulting in hemogenic clusters that undergo apoptosis.

Transcriptional profiling of the *Chd1* mutant endothelium reveals an early loss of the hematopoietic program

To assess the transcriptional consequences of *Chd1* loss in endothelial cells, we conducted global gene expression analyses of $CD31^+$ endothelial cells isolated from whole E10.5 embryos. Four biological replicates each of CreHet and mutant E10.5 $CD31^+$ $tdTomato^+$ cells were processed for microarray analyses. We found that only a small number of genes are affected in the mutants: 196 genes, at $p<0.01$ and a log2 fold-change of 0.4 or more (Figure 6A). Thus, the vast majority of the transcriptional

program of the E10.5 endothelium is unaffected in the mutants. Significantly more genes are down-regulated (156 genes) than up-regulated (40 genes) in the mutant endothelium (Figure 6B), consistent with previous reports that mouse Chd1 associates with the promoters of active genes and serve as a positive regulator of transcription (Gaspar-Maia et al., 2009; Guzman-Ayala et al., 2015).

Gene ontology analysis revealed that the set of genes down-regulated in the mutants is remarkably enriched for functions in hematopoiesis and the immune system (Figures 6C and 6D). We analyzed this dataset further using an unbiased gene set enrichment analysis (GSEA) (Subramanian et al., 2005) and observed similar enrichments for immune-related functions (Figure S6A). In addition, we identified very significant enrichments for genes regulated by Gata2 and Runx1-Runx1t1 (Figures S6B and S6C), and both of these transcription factors are key regulators of the emergence of HSPCs (Chen et al., 2009; de Pater et al., 2013).

Our results are in agreement with three recent studies showing that the emergence of HSPCs is regulated by immune/inflammatory response (Espín-Palazón et al., 2014; Li et al., 2014; Sawamiphak et al., 2014). In one of the studies, Li and colleagues carried out expression profiling of $CD31^{+}$ $Cdh5^{+}$ $Esam^{+}$ $Ly6a\text{-}GFP^{+}$ Kit^{+} hematopoietic cluster cells (HCCs) compared to endothelial cells (ECs). Interestingly, Chd1 is a member of “Cluster 1”, which includes the genes identified by Li et al. as up-regulated in HCCs (Figure S6D) (Li et al., 2014). Further analysis of the gene expression data segregated via the Li et al. subsets revealed a specific loss of HCC-

associated genes and a corresponding enrichment of EC-associated genes in *Chd1*-deficient endothelium (Figure 6E).

The lower detection of hematopoiesis genes in mutant $CD31^+$ endothelial cells could be due to reduced levels of expression per cell, or reduced numbers of early hematopoietic cells that are still $CD31^+$. The latter possibility is more likely, given the lower numbers of $CD31^+$ $Ter119^-$ Kit^+ $CD45^+$ cells in E10.5 mutants (Figures 5D and 5E). Taken together, our results indicate that Chd1 is essential for the establishment of an HSPC-associated transcriptional sub-program in cells emerging from the E10.5 endothelium, potentially by promoting their survival and expansion. This transcriptional sub-program is anticipated to be a useful resource for the discovery of novel markers or regulators of definitive hematopoiesis in future studies.

Chd1-dependent elevation in transcriptional output in emerging HSPCs

We recently found that Chd1 promotes an elevated transcriptional output essential for optimal self-renewal of ES cells and growth of the epiblast (Guzman-Ayala et al., 2015). ES cells are known to be in a state of hyper-transcription, with a global elevation of transcriptional output per cell (Efroni et al., 2008). We found that *Chd1*$^{-/-}$ ES cells express lower levels of most mRNAs, intergenic transcripts and ribosomal RNA on a per-cell basis, and these defects are associated with reduced recruitment of RNA Pol II to active genes (Guzman-Ayala et al., 2015). Thus, Chd1 promotes global

transcriptional amplification of both mRNAs and rRNA, in a manner similar to that reported for Myc (Lin et al., 2012; Nie et al., 2012). Interestingly, we noticed that genes validated as Myc targets, as well as ribosomal protein genes, are preferentially down-regulated in *Chd1* mutant CD31$^+$ samples (Figures 7A, 7B and S7). These results raised the question of whether the levels of transcriptional output are increased in emerging HSPCs. prompted us to explore the levels of transcriptional output in emerging HSPCs. This is a challenging question to answer, given the rare nature of these cells, and has not to our knowledge been addressed before.

We examined the global nascent RNA transcription levels of E11.5 AGM cells by incorporation of 5-ethynyl-uridine (EU), and found that tdTomato$^+$ CD31$^+$ Kit$^-$ structural endothelial cells maintain a similar RNA transcriptional output as tdTomato$^-$ CD31$^-$ Kit$^-$ non-endothelial cells in control AGMs (Figure 7C). Remarkably, tdTomato$^+$ CD31$^+$ Kit$^+$ hematopoietic cluster cells in CreHet AGMs exhibit an elevated rate of nascent RNA synthesis, incorporating on average 75.3% more EU per cell when compared to tdTomato$^+$ CD31$^+$ Kit$^-$ structural endothelium (Figures 7C and 7D, n=7 CreHets). This increase is also observed in tdTomato$^+$ CD45$^+$ cells, with an average of 79.2% higher EU incorporation per cell compared to tdTomato$^+$ CD31$^+$ Kit$^-$ cells (Figures 7C and 7D).

We next examined *Chd1* mutant AGM cells, and found that mutant tdTomato$^-$ CD31$^-$ Kit$^-$ and tdTomato$^+$ CD31$^+$ Kit$^-$ cells have normal levels of global transcriptional output compared to the corresponding sub-populations in the CreHet AGM (Figure 7E). Thus, the deletion of *Chd1* does not appear to affect the global transcriptional output of structural endothelium. However, the elevated transcriptional output observed in CreHet

tdTomato^{+} CD31^{+} Kit^{+} cells is significantly suppressed in mutant cells (35.8% compared to tdTomato^{+} CD31^{+} Kit^{-} cells, p=0.0077, n=4 mutants) (Figures 7C, 7D and 7E). The increase in transcriptional activity in tdTomato^{+} CD45^{+} cells is similarly suppressed in the mutants (41.3% compared to tdTomato^{+} CD31^{+} Kit^{-} cells, p=0.0134) (Figures 7C, 7D and 7E). Taken together, these results indicate that the differentiation of CD31^{+} Kit^{-} endothelium to CD31^{+} Kit^{+} hematopoietic cluster cells and CD45^{+} blood cells in the E11.5 AGM coincides with an elevation in total nascent transcriptional output, and this increase is Chd1-dependent.

Chd1 is not required for blood development after HSPC specification

The data above are consistent with a requirement for *Chd1* in the transition of endothelial cells into HSPCs. However, it remained possible that the defects observed were due to a role of Chd1 after HSPC specification (Figure 5A). To determine whether *Chd1* is required for hematopoietic development after the endothelial-to-hematopoietic transition, we deleted *Chd1* specifically in hematopoietic cells using *Vav-Cre* (de Boer et al., 2003). This Cre line is active in HSPCs and their progeny in the embryo proper as early as E11 (Padrón-Barthe et al., 2014). In contrast to the deletion of *Chd1* within the endothelial compartment, normal Mendelian ratios of live pups were observed at birth upon hematopoietic-specific deletion (Table 1). *Vav-Cre* mutant embryos do not display any signs of fetal liver anemia (data not shown), and the size of mutant E13.5 FLs is comparable to that of littermate controls (Figure 8A). Consistent with these

observations, *Vav-Cre* mutant FL cells show no defect in erythroid development in methylcellulose culture assays (CFU-E) (Figure 8B). Moreover, an analysis of peripheral blood composition of control and mutant mice at 1 year of age revealed complete recombination of the *Chd1*^{flox} allele at the genomic DNA level (Figure 8C) but no significant differences in all of the major blood populations examined, namely CD11b^{+} GR-1^{+} SSC^{hi} granulocytes, CD11b^{+} GR-1^{+} SSC^{int} monocytes, CD11b^{+} GR-1^{-} macrophages, CD19^{+} B cells, TCRβ^{+} CD4^{+} T cells, TCRβ^{+} CD8^{+} T cells, and TCRβ^{-} NK1.1^{+} NK cells (Figure 8D, n=6 mutants vs n=6 CreHets). Taken together, these results indicate that Chd1 is not required for hematopoietic development and homeostasis after HSPC specification.

Discussion

Recent studies traced the origin of the adult hematopoietic system to a small number of hemogenic endothelial cells found associated with mid-gestational arteries. However, the low percentage of endothelial cells that differentiates into hematopoietic cells and the technical difficulty in isolating these hemogenic clusters results in limited material available for analysis. Consequently, very little is known about how the endothelial-to-hematopoietic transition occurs in vivo, and only a few genes or pathways, including *Runx1* (Chen et al., 2009), *Gata2* (de Pater et al., 2013), Notch signaling (Kumano et al., 2003), and the Wnt/β-catenin pathway (Ruiz-Herguido et al., 2012), have been implicated in this process. Our study documents that Chd1 is the first chromatin remodeler shown to be essential for the emergence of HSPCs from the endothelium. We further define the specific temporal window of requirement for Chd1 and identify a transcriptional sub-program associated with HSPCs and cellular growth that is lacking in *Chd1* mutants. Finally, we identify an elevation in transcriptional output during the transition of endothelium to hematopoietic progenitors, and this elevation is Chd1-dependent. These results indicate that chromatin remodeling is key to emergence of HPSCs from the endothelium, and provide insight into the underlying molecular mechanisms.

Intra-aortic hematopoietic clusters form in the *Chd1* mutant AGM and express Runx1 and Kit, but the mutant clusters show signs of apoptotic cell death and a failure to mature into $CD45^{+}$ hematopoietic cells. These results place the function of Chd1

downstream of the requirement for Wnt/β-catenin activity (Ruiz-Herguido et al., 2012) and upstream of the activation of CD45. These data indicate that the earliest definitive hematopoietic progenitors form in *Chd1* mutants but fail to expand in numbers and instead are lost by apoptosis. While Chd1 is not required for subsequent differentiation of HSPCs and steady-state maintenance of the adult hematopoietic system, it remains possible that Chd1 plays a functional role upon acute infection, regeneration or aging.

Note that Chd1 is not required for baseline levels of transcription to occur, as evidenced by our analysis of transcriptional output in structural endothelium (Fig. 7), and the fact that both *Chd1* mutant endothelium and *Vav-Cre* induced mutant hematopoietic cells develop normally. Our results indicate that Chd1 drives an elevated transcriptional output that is specifically required for survival and expansion of HSPCs emerging from the endothelium. There are about 400-500 Kit^+ cells in the dorsal aorta at E10.5 (Chen et al., 2009), and only a subset of these are HSPCs (Boisset et al., 2014; Li et al., 2014). The fact that HSPCs arise from such a rare fraction of the endothelium and need to rapidly give rise to the entire definitive blood system is expected to generate a high demand for cellular growth pathways, including transcription and translation. Cell doubling times of as low as 8 hours have been described for fetal erythroblasts (Paul et al., 1972), and we see a decrease of cell cycle entry in *Chd1* mutants within the fetal liver cell compartment which is comprised of a large subset of erythroblasts (Figure 3F). The higher expression of *Chd1* in HSPCs (Li et al., 2014) and the data demonstrating that Chd1 is required for the up-regulation of HSPC-associated genes, Myc targets, ribosomal protein genes and overall transcriptional output during the endothelium-to-

hematopoietic transition, all support the model that cellular growth pathways dependent on Chd1 are key to HSPC survival and expansion (Figure 9). Chd1 is required for Myc-driven hyper-proliferation in mammary cells (Kessler et al., 2012), and both Chd1 and Myc promote a globally elevated transcriptional output in ES cells (Guzman-Ayala et al., 2015; Lin et al., 2012; Nie et al., 2012). At the biochemical level, Chd1 removes the promoter-proximal nucleosomal barrier and facilitates the engagement of RNA Pol II with elongation (Skene et al., 2014). In addition to enhancing the expression of RNA Pol II genes, Chd1 is also a direct regulator of the output of ribosomal RNA (Guzman-Ayala et al., 2015). Of note, deficiencies in ribosomal protein genes can cause anemia and other blood disorders (Teng et al., 2013). It will therefore be of interest to assess the transcriptional and protein output of HSPCs at the single-cell level. The recent development of tools to enrich for different cellular fractions along the transition between endothelium and HSPCs (Li et al., 2014), and to perform ChIP-seq with low numbers of freshly collected embryonic cells (Sachs et al., 2013), paves the way for the dissection of the chromatin and transcriptional reprogramming events that lead to the emergence of HSPCs. These studies may in turn inform the development of improved methods to generate HSPCs in vivo or expand them ex vivo for applications in Regenerative Medicine. Moreover, it will be of interest to explore whether modulations of global transcriptional output also have a regulatory role in other stem cell systems, in particular those with rapidly expanding progenitor cells during normal development or cancer.

Figure 2. Deletion of *Chd1* in the endothelium leads to fetal liver anemia and lethality at mid-gestation.

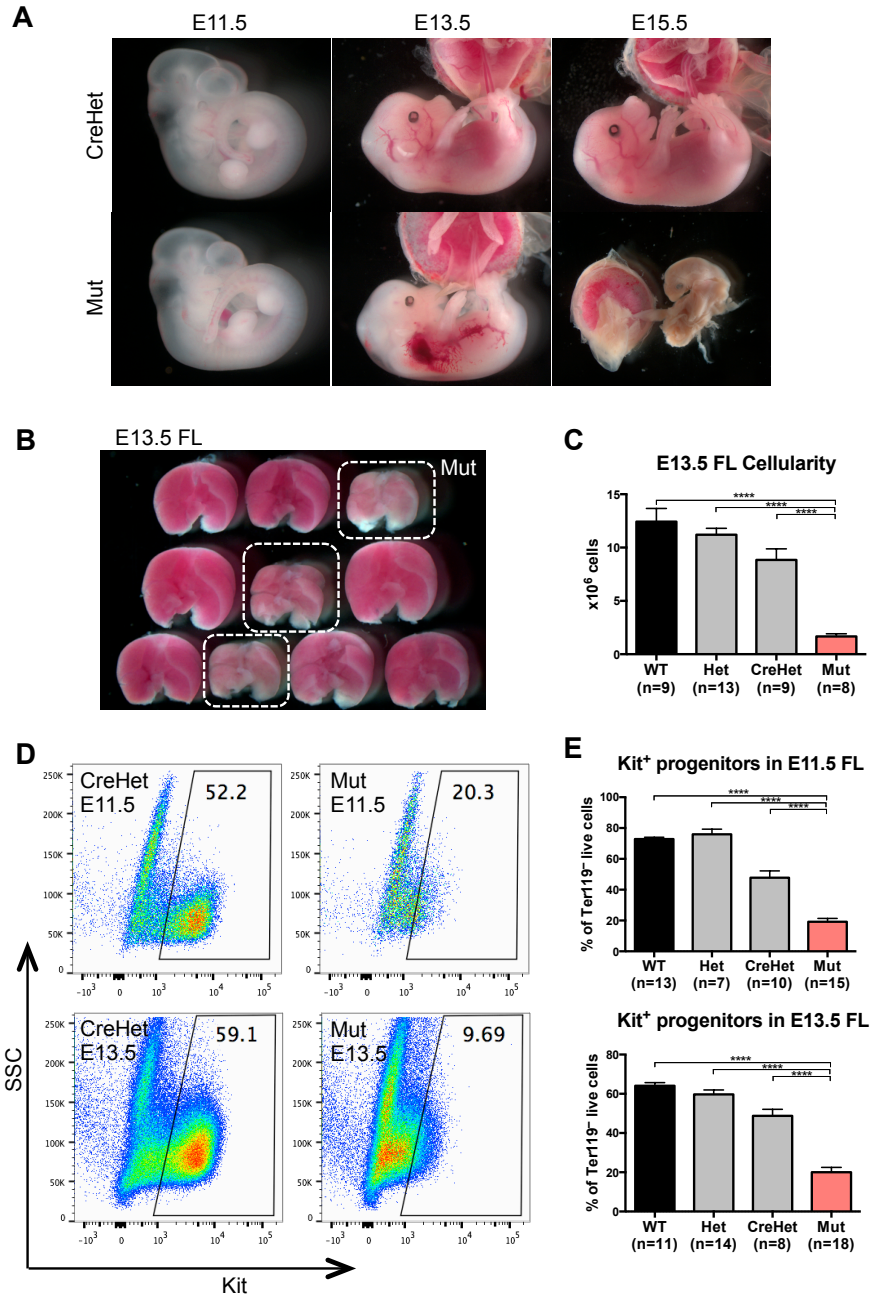

Figure 2. Deletion of *Chd1* in the endothelium leads to fetal liver anemia and lethality at mid-gestation.

(A) Representative images of CreHet control and mutant embryos at various embryonic stages. Mutant embryos appear normal at E11.5, but are pale and exhibit hemorrhage and edema by E13.5. Mutants are resorbed by E15.5.

(B) Representative image showing dissected FLs from a litter of E13.5 embryos. The three mutant livers (circled in white) are paler and smaller compared to littermate controls.

(C) E13.5 FLs from mutant embryos are significantly smaller than from controls. n=5 litters. Error bars indicate s.e.m..

(D) Representative flow plots show that mutant FL contains fewer Kit^+ progenitors at E11.5 and E13.5 compared to controls.

(E) Quantification of Kit^+ cells at both E11.5 and E13.5. E11.5: n=7 litters. E13.5: n=8 litters. Error bars indicate s.e.m..

Figure 3. Failure of definitive erythropoiesis in *Chd1* mutants.

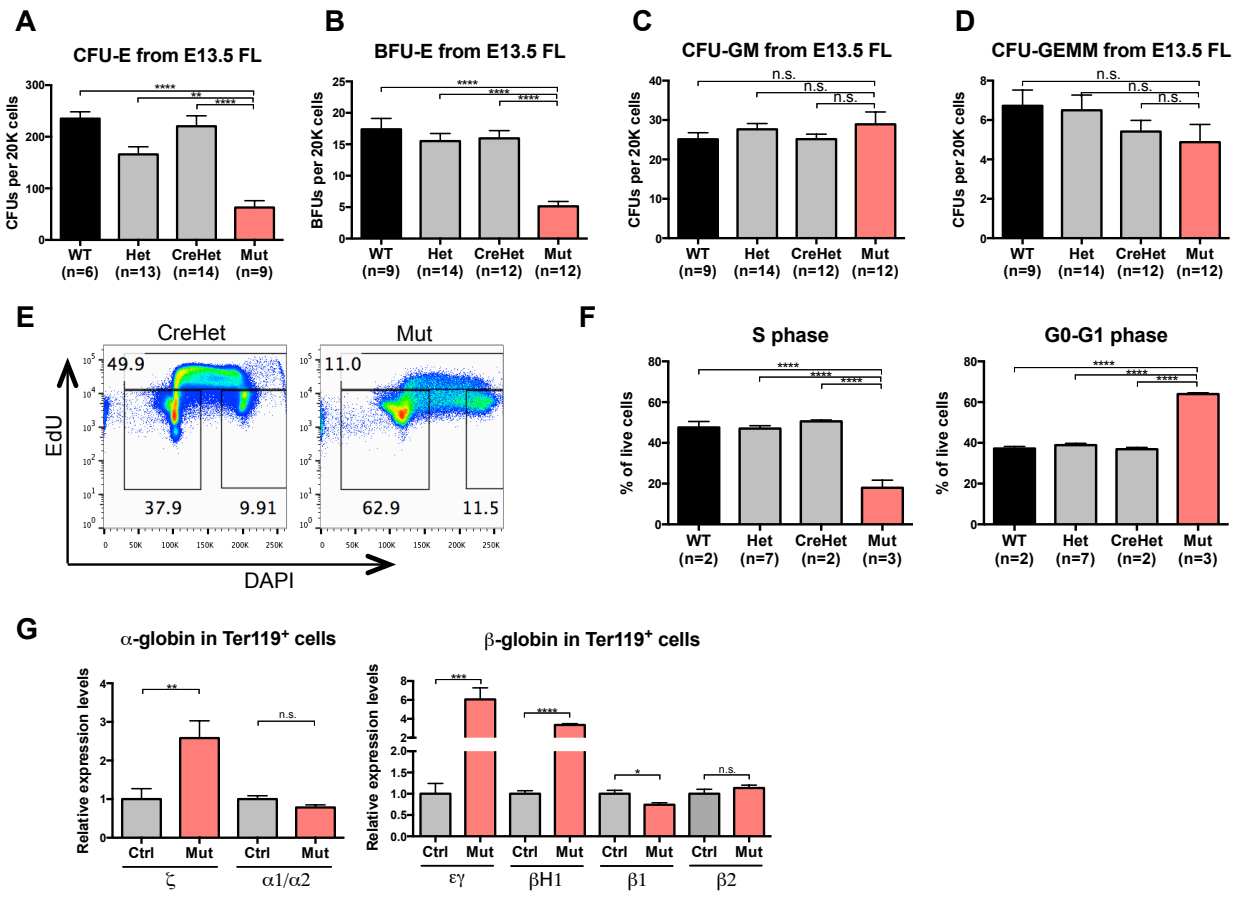

Figure 3. Failure of definitive erythropoiesis in *Chd1* mutants.

(A) CFU-E colony counts from 20,000 FL cells per E13.5 embryo seeded, in duplicates. n= 5 litters. Error bars indicate s.e.m..

(B-D) BFU-E, CFU-GM and CFU-GEMM colony counts from 20,000 FL cells per E13.5 embryo seeded, in duplicates. n=6 litters. Error bars indicate s.e.m..

(E) Representative flow plots show reduced EdU incorporation in mutant FL at E13.5.

(F) Quantification showing a strong reduction of FL cells in S phase and a corresponding increase of cells in G0-G1 phase in mutant FL. n=2 litters. Error bars indicate s.e.m..

(G) qRT-PCR of sorted $Ter119^{+}$ cells from E13.5 FLs show an increase of primitive erythroid globins and a reduction of definitive erythroid globins. n=8 control and 5 mutant embryos from 3 litters. Error bars indicate s.e.m..

Figure 4. *Chd1* mutant FLs are deficient in Ter119^{-} Kit^{+} Sca1^{+} hematopoietic stem and progenitor cells.

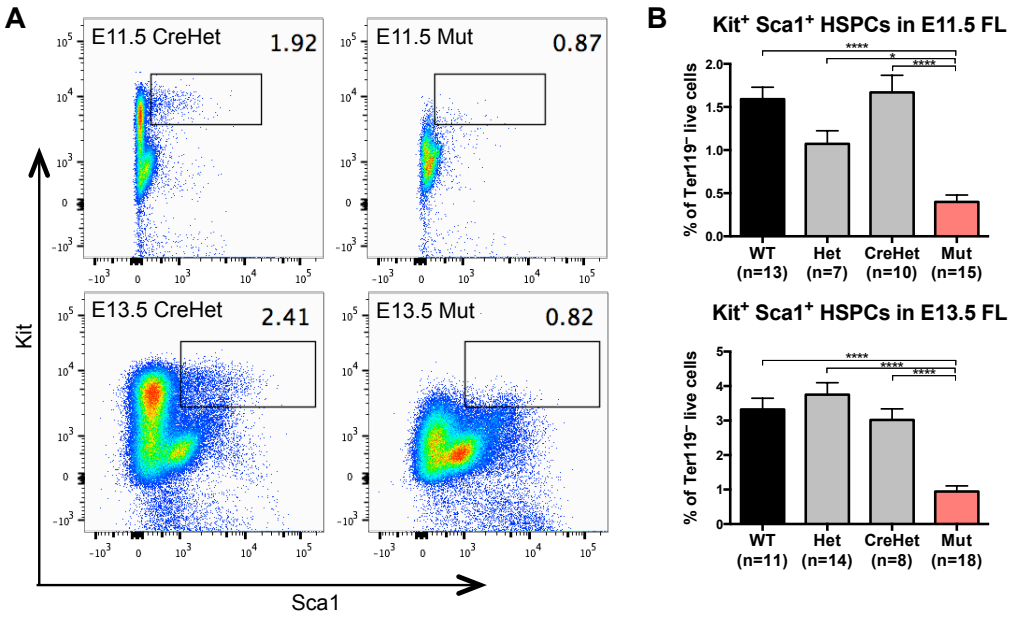

Figure 4. *Chd1* mutant FLs are deficient in Ter119^{-} Kit^{+} Sca1^{+} hematopoietic stem and progenitor cells.

(A) Representative flow plots show a loss of Ter119^{-} Kit^{+} Sca1^{+} cells in mutant E11.5 and E13.5 FLs.

(B) Kit^{+} Sca1^{+} HSPCs are significantly reduced in mutant compared to control FL at both E11.5 and E13.5. E11.5: n=7 litters. E13.5: n=8 litters. Error bars indicate s.e.m..

Figure 5. *Chd1* mutant AGM contains intra-aortic hematopoietic clusters that do not mature to blood cells in vivo and in vitro.

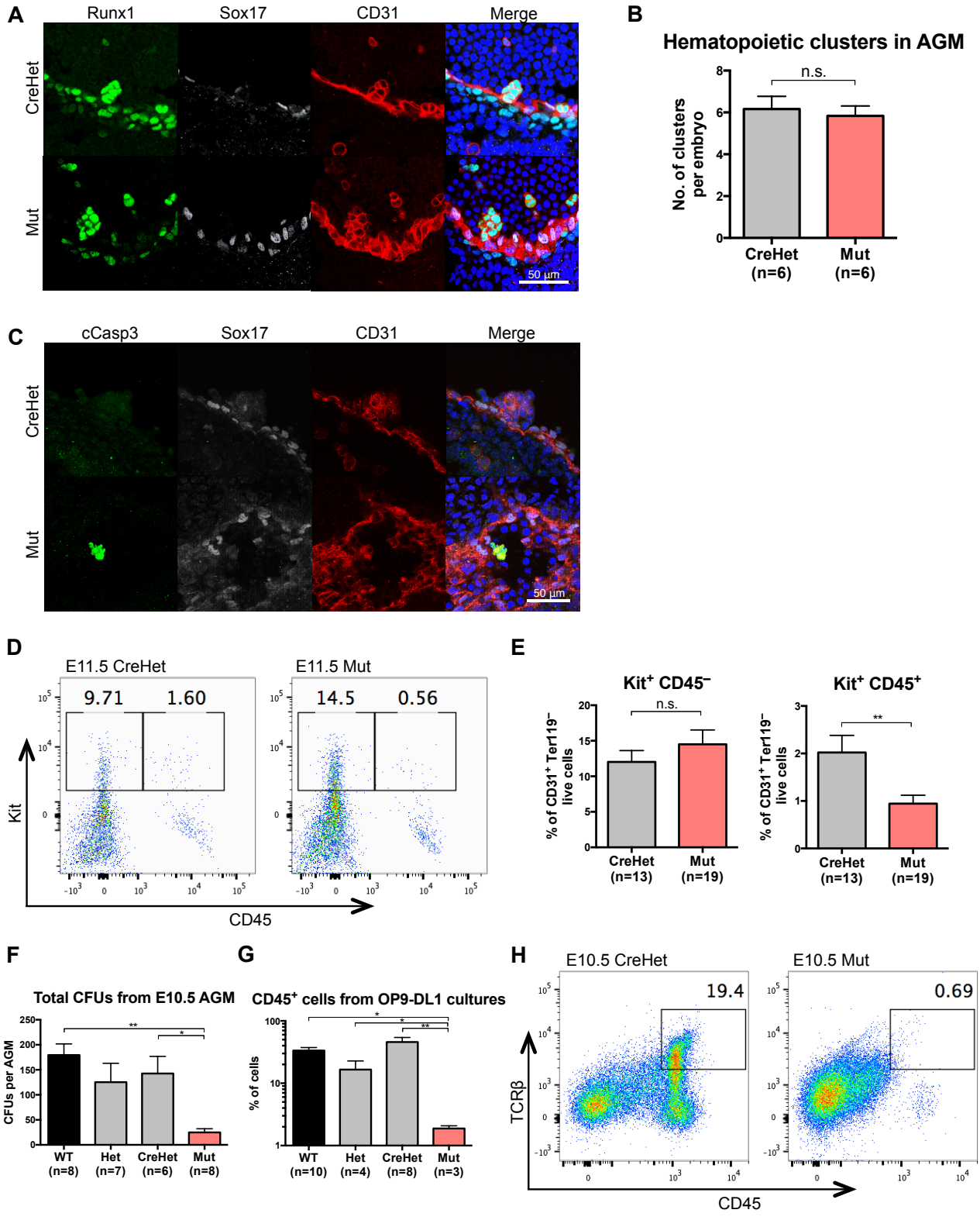

Figure 5. *Chd1* mutant AGM contains intra-aortic hematopoietic clusters that do not mature to blood cells in vivo and in vitro.

(A) Intra-aortic clusters in the E10.5 AGM show proper expression of Runx1 and CD31, and the absence of arterial marker Sox17.

(B) Mutant AGMs show similar numbers of hemogenic clusters compared to CreHets. n=6 mutants and 6 CreHets from 3 litters.

(C) Intra-aortic clusters in mutant E10.5 AGMs stain positive for cleaved caspase-3 (cCasp3), a marker for apoptosis, which is not detected in clusters from CreHet AGMs. n=3 mutants and 2 CreHet embryos.

(D) Representative flow plots of $Ter119^{-}$ $CD31^{+}$ cells show a loss of Kit^{+} $CD45^{+}$ cells in E11.5 mutant AGMs.

(E) $CD31^{+}$ $Ter119^{-}$ cells from mutant E11.5 AGMs contains a comparable Kit^{+} $CD45^{-}$ population, but show a significant reduction of Kit^{+} $CD45^{+}$ cells compared to CreHets. n= 7 litters.

(F) Total CFU colony counts from E10.5 AGM, in duplicates. n=4 litters.

(G) Mutant AGMs are highly defective in the generation of $CD45^{+}$ cells when co-cultured with OP9-DL1 stromal cells. n=4 litters.

(H) Representative flow plots show that mutant AGMs do not give rise to $CD45^{+}$ $TCR\beta^{+}$ T cells when co-cultured with OP9-DL1 stromal cells.

Figure 6. Reduced expression of hematopoietic and growth genes in the E10.5 *Chd1* mutant endothelium.

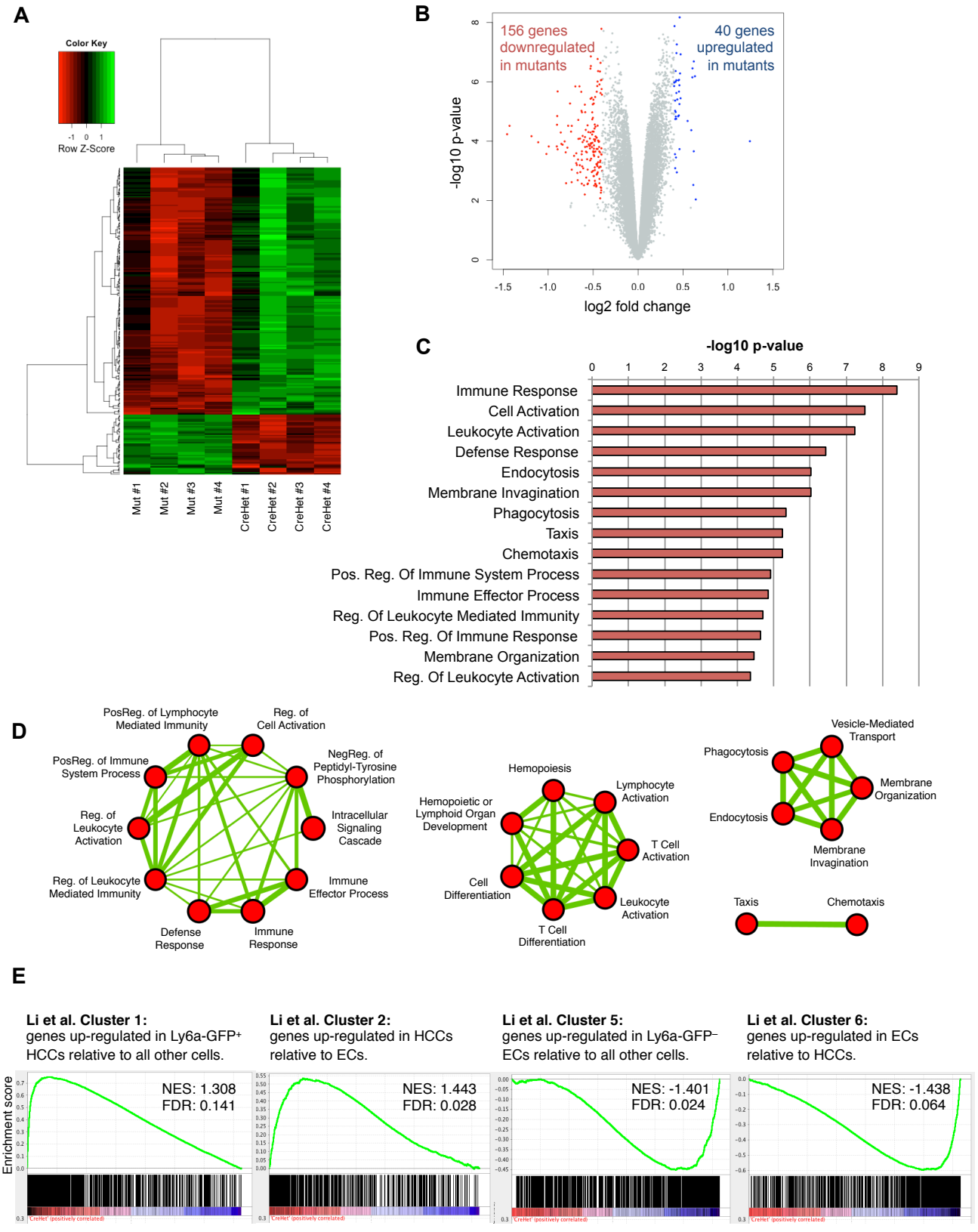

Figure 6. Reduced expression of hematopoietic and growth genes in the E10.5 *Chd1* mutant endothelium.

(A,B) Microarray analysis comparing 4 biological replicates each of CreHet and mutant endothelium at E10.5 shows a mild mis-regulation of gene expression. Cut-off of $p < 0.01$ and $| logFC | > 0.4$ is depicted.

(C) DAVID Gene Ontology analysis shows that immune-related categories are significantly enriched in the set of genes down-regulated in the *Chd1* mutant endothelium. Similar results were obtained when all differentially expressed genes were used.

(D) GO enrichment analysis shows that GO terms fall into 4 main clusters. Thickness of connecting lines represents the number of shared genes underpinning the two connected terms.

(E) GSEA for gene clusters identified by Li et al. as differentially expressed between hematopoietic cluster cells (HCCs) and endothelial cells (ECs) shows that HCC-upregulated genes are preferentially decreased and EC-upregulated genes are preferentially increased in *Chd1* mutant endothelium. (PMID: 25395663) NES: net enrichment score. FDR: false discovery rate.

Figure 7. Chd1 is required for elevated RNA transcription in the hemogenic endothelium.

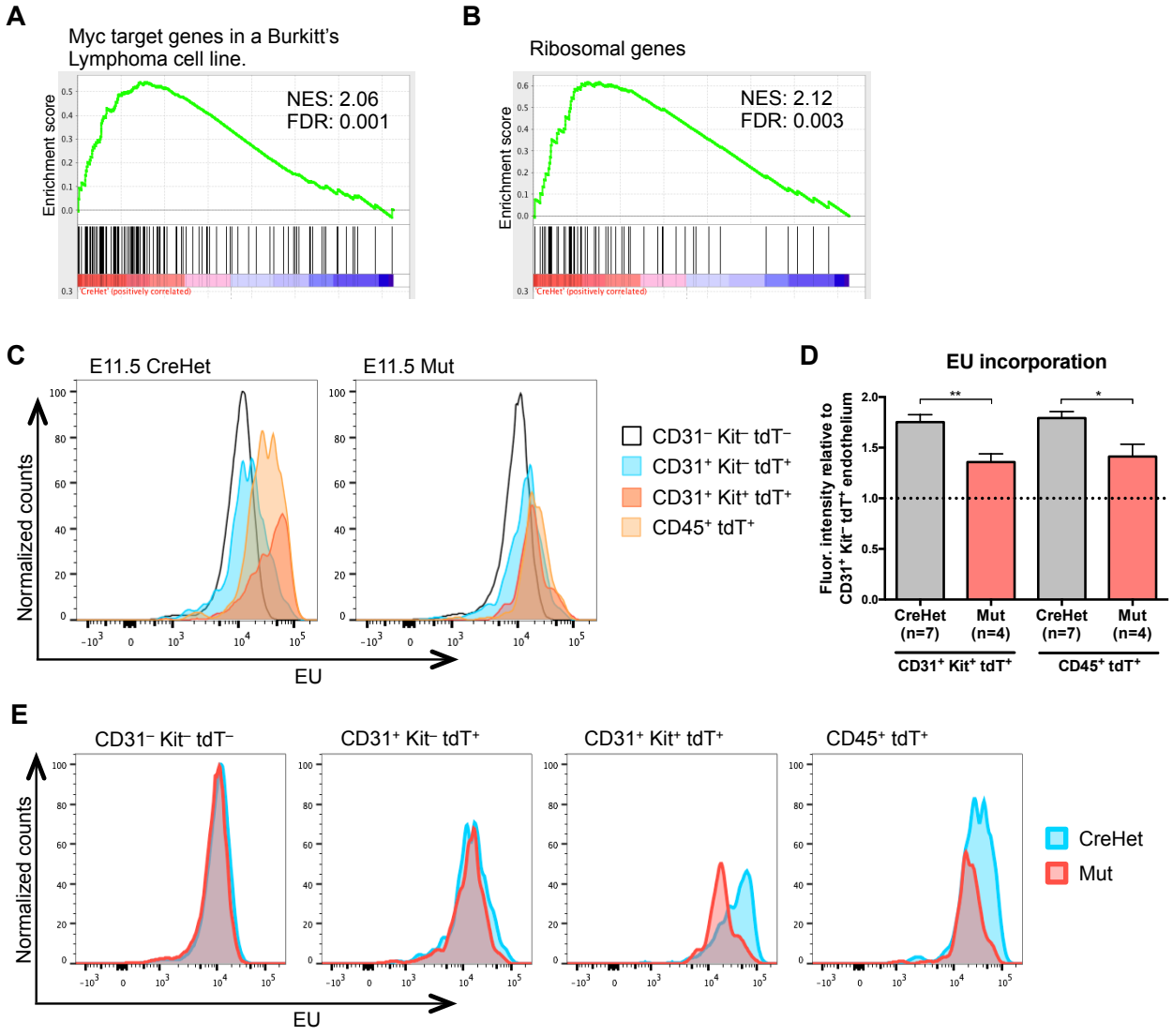

Figure 7. Chd1 is required for elevated RNA transcription in the hemogenic endothelium.

(A) GSEA for genes up-regulated by Myc and whose promoters are bound by MYC, via phylogenetic comparison and ChIP in P493 cells (PMID: 14519204) reveals a preferential loss of Myc targets in *Chd1* mutant endothelium. NES: net enrichment score. FDR: false discovery rate.

(B) GSEA for genes listed in KEGG Pathway for "Ribosome" reveals a preferential down-regulation in *Chd1* mutant endothelium.

(C) Normalized histograms of EU incorporation reveal distinct levels of nascent transcriptional output between different sub-populations in the E11.5 AGM.

(D) Both $CD31^{+}$ Kit^{+} and $CD45^{+}$ cells incorporate higher levels of EU compared to $CD31^{+}$ Kit^{-} endothelium in controls. This increase is significantly suppressed in mutant cells. Error bars indicate s.e.m..

(E) Normalized histograms of EU incorporation reveal that mutant cells have levels of transcriptional output similar to controls in $CD31^{+}$ Kit^{-} E11.5 AGM endothelium but are defective in the up-regulation of nascent RNA transcription in $CD31^{+}$ Kit^{+} and $CD45^{+}$ cells.

Note that all cells in the EU incorporation analyses of (C)-(E) are also $tdTomato^{+}$, i.e. derived from the Tie2/Cre-marked lineage, with the exception of $CD31^{-}$ Kit^{-} cells.

Figure 8. Hematopoietic-specific *Chd1* mutants are viable and phenotypically normal.

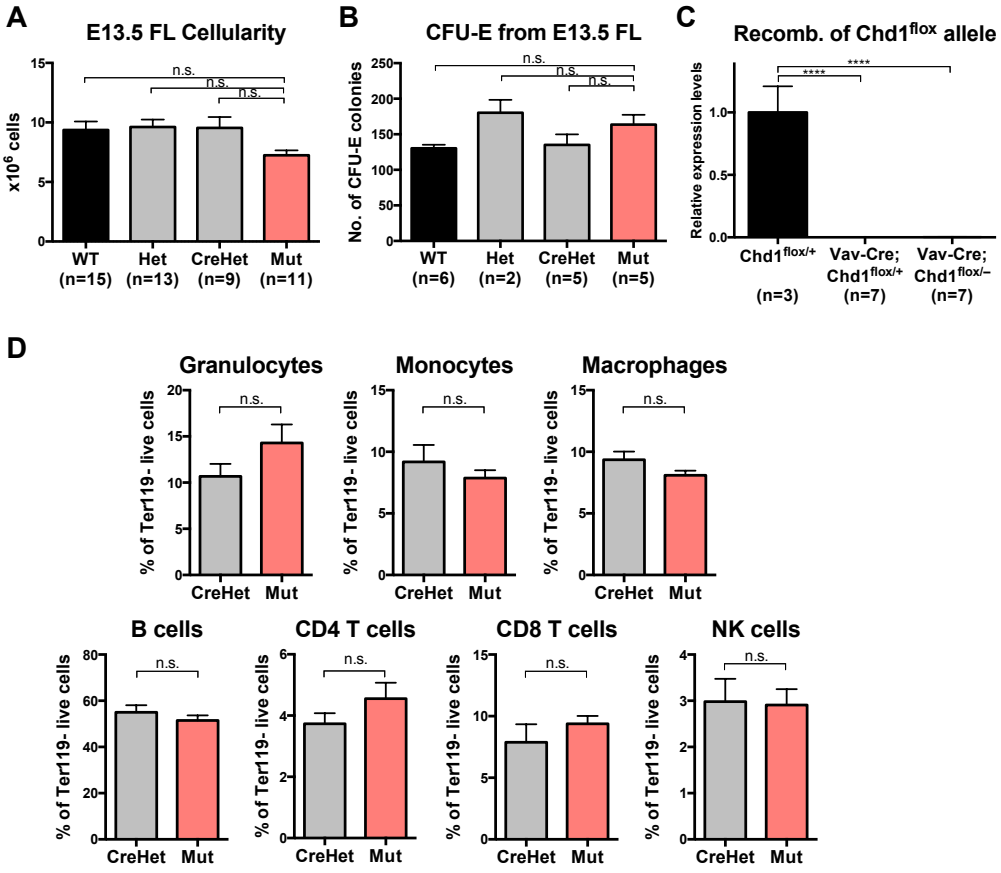

Figure 8. Hematopoietic-specific *Chd1* mutants are viable and phenotypically normal.

(A) Fetal livers from mutant embryos generated using *Vav-Cre* contain similar cell numbers to littermate controls. n=6 litters. Error bars indicate s.e.m..

(B) CFU-E colony counts for mutant livers appear comparable to those from controls. n=2 litters. Error bars indicate s.e.m..

(C) Intact $Chd1^{flox}$ allele is undetectable in the peripheral blood of *Vav-Cre* adult animals. Error bars indicate s.e.m..

(D) Peripheral blood from mutant mice and CreHet controls shows comparable blood populations at one year of age. n=6 CreHet and 6 mutants from 6 litters. Error bars indicate s.e.m..

Figure 9. Model for the role of Chd1 in transcriptional output and emergence of HSPCs.

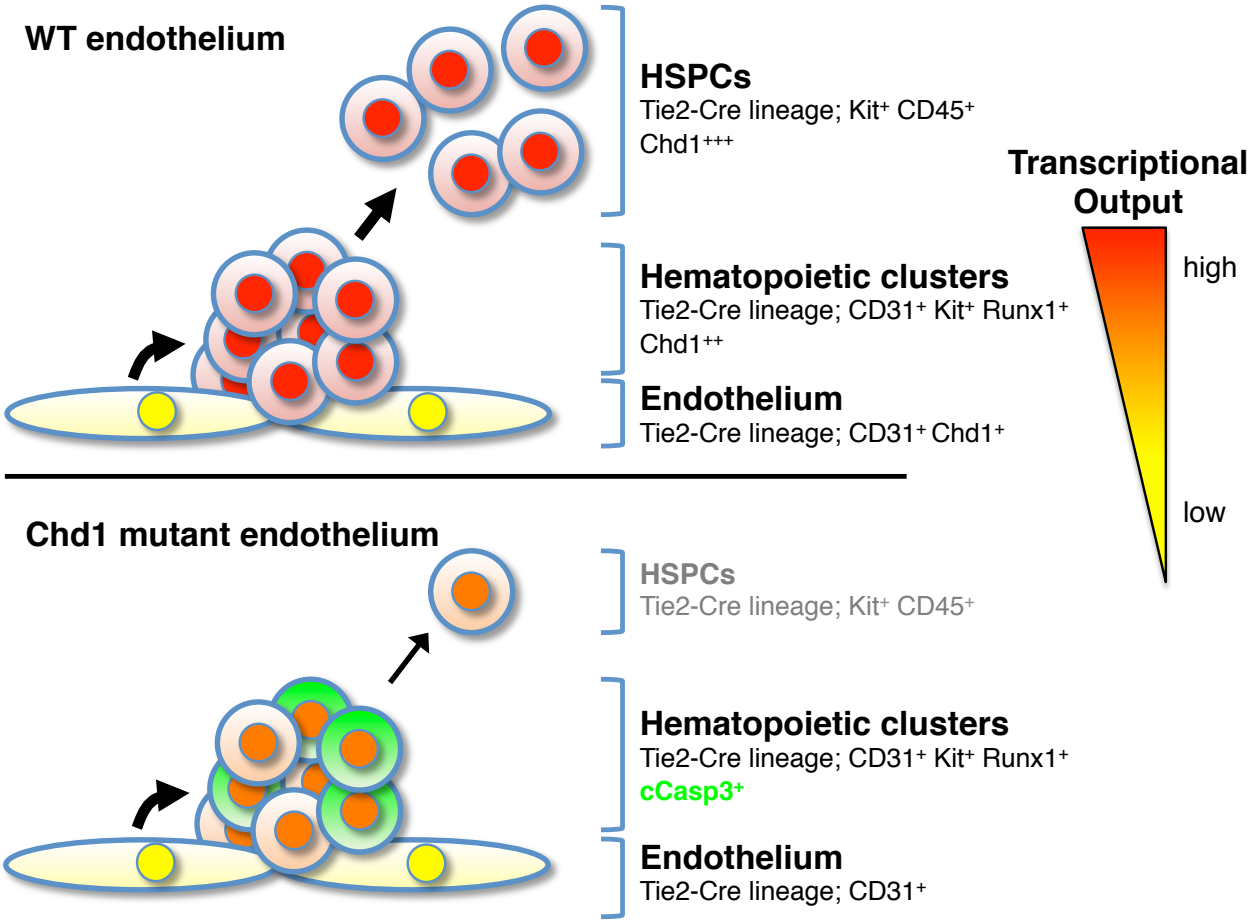

Figure 9. Model for the role of Chd1 in transcriptional output and emergence of HSPCs.

The expression of Chd1 and the levels of nascent transcriptional output are increased in hematopoietic progenitors relative to endothelium. Deletion of Chd1 from the endothelium allows the formation of hematopoietic clusters, but these have reduced levels of transcriptional output, fail to expand and are lost by apoptosis. See text in Chapter 2 for details.

Figure S1. *Chd1* is broadly expressed in the mid-gestational mouse embryo.

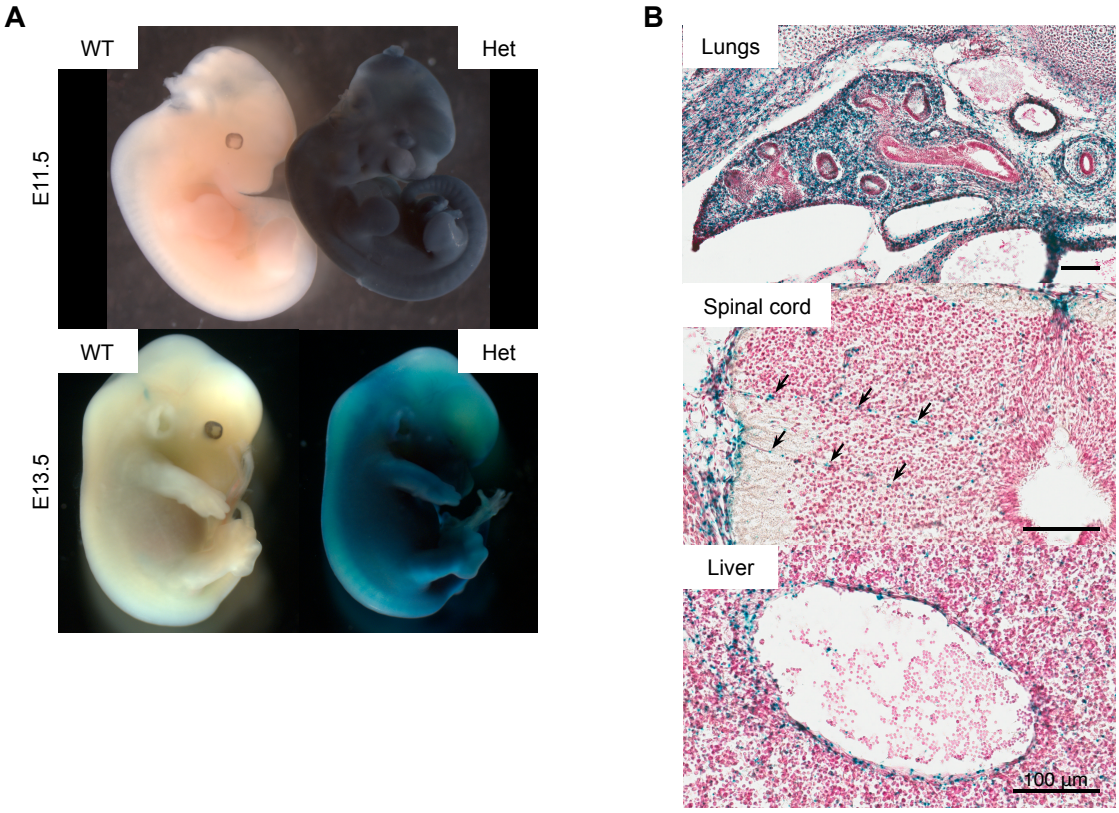

Figure S1. *Chd1* is broadly expressed in the mid-gestational mouse embryo.

(A) Whole-mount X-gal staining of $Chd1^{LacZ}$ embryos indicates a broad expression of *Chd1* in E11.5 and E13.5 embryos.

(B) $Chd1^{LacZ}$ is expressed in the endothelium in various tissues in the E13.5 embryo, including in the lungs, intramedullary blood vessels in the spinal cord (black arrows), and in the ductus venosus in the FL. Scale bar represents 100 μm.

Figure S2. High recombination efficiency and normal development of the vasculature in endothelial *Chd1* mutants.

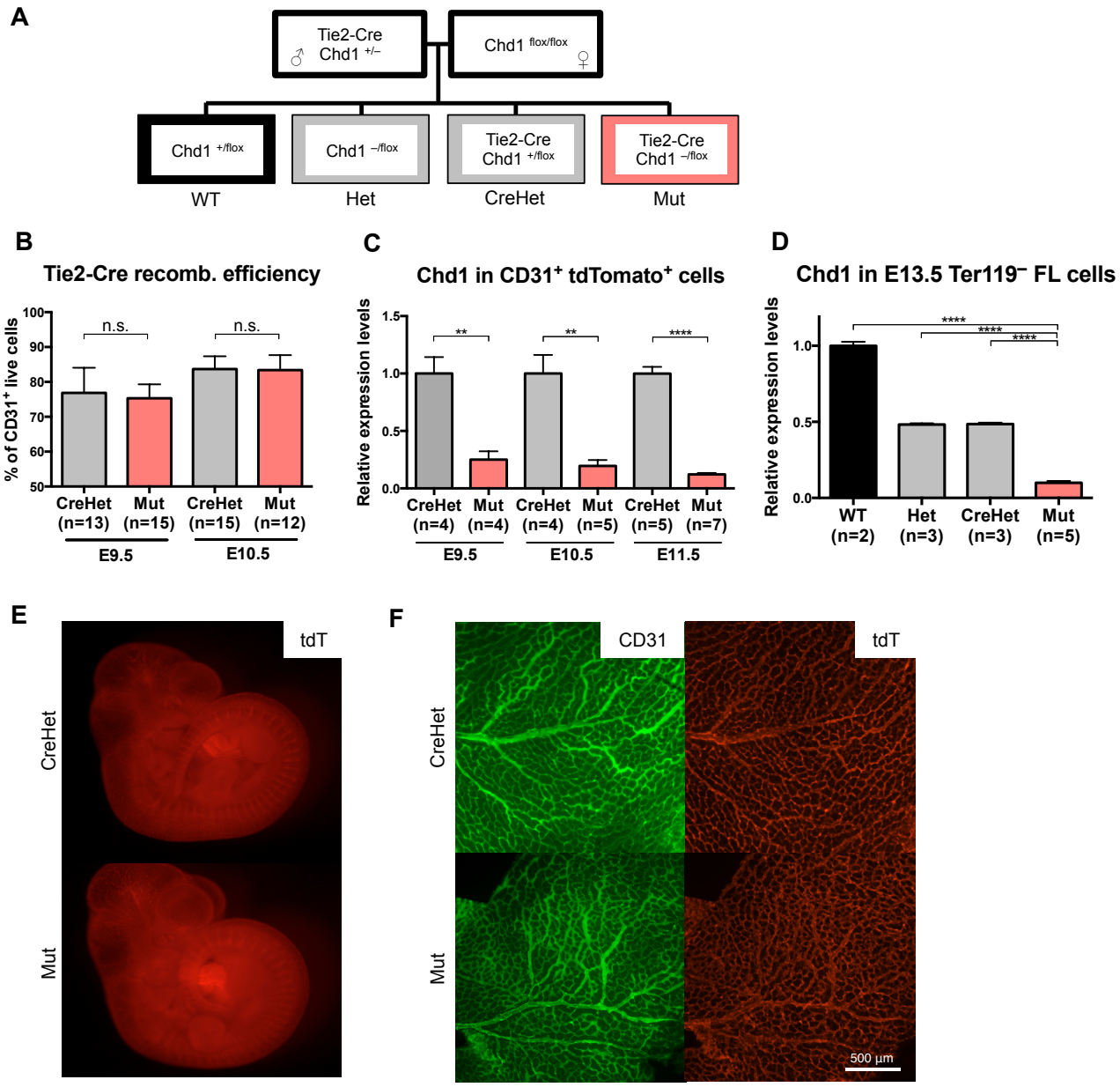

Figure S2. High recombination efficiency and normal development of the vasculature in endothelial *Chd1* mutants.

(A) Mouse breeding scheme used to generate Tie2-Cre; $Chd1^{-/flox}$ mutant embryos. 1 in 4 embryos are expected to be of the mutant genotype.

(B) Tie2-Cre is an efficient Cre deletor line, achieving 76% recombination in E9.5 $CD31^{+}$ cells, and a significantly higher 84% at E10.5 ($p<0.0001$). Recombination efficiency is not significantly different between CreHet controls and mutants at either stage. Error bars indicate s.e.m..

(C,D) qRT-PCR analyses document the loss of *Chd1* expression in $CD31^{+}$ $tdTomato^{+}$ cells at E9.5, E10.5 and E11.5, and in E13.5 $Ter119^{-}$ FL cells.

(E) tdTomato reporter marks the extensive Cre recombination within the embryonic vasculature in E11.5 embryos.

(F) Whole-mount immunofluorescence of E10.5 CreHet and mutant yolk sacs shows a normal endothelial network.

Figure S3. Normal heart development but evidence of anemia in endothelial *Chd1* mutants.

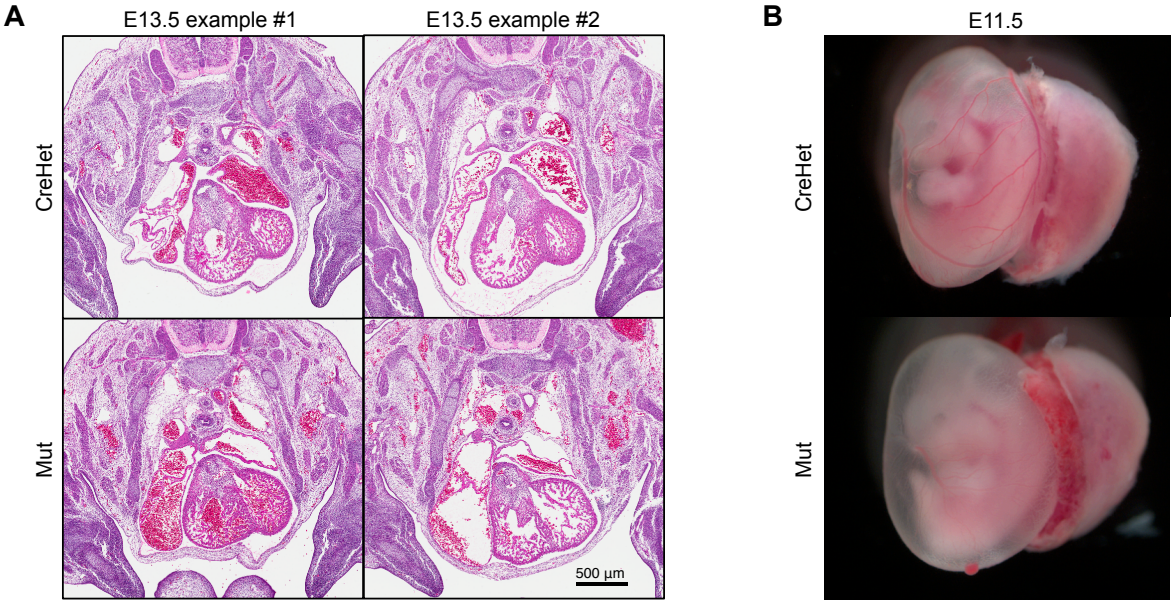

Figure S3. Normal heart development but evidence of anemia in endothelial *Chd1* mutants.

(A) 4-chamber heart view transverse sections of CreHet and mutant hearts at E13.5 show no visible defects in heart chamber formation.

(B) Yolk sacs of mutant E11.5 embryos appear anemic immediately after removal from the decidua.

Figure S4. Endothelial *Chd1* mutants display blood within lymphatic vessels.

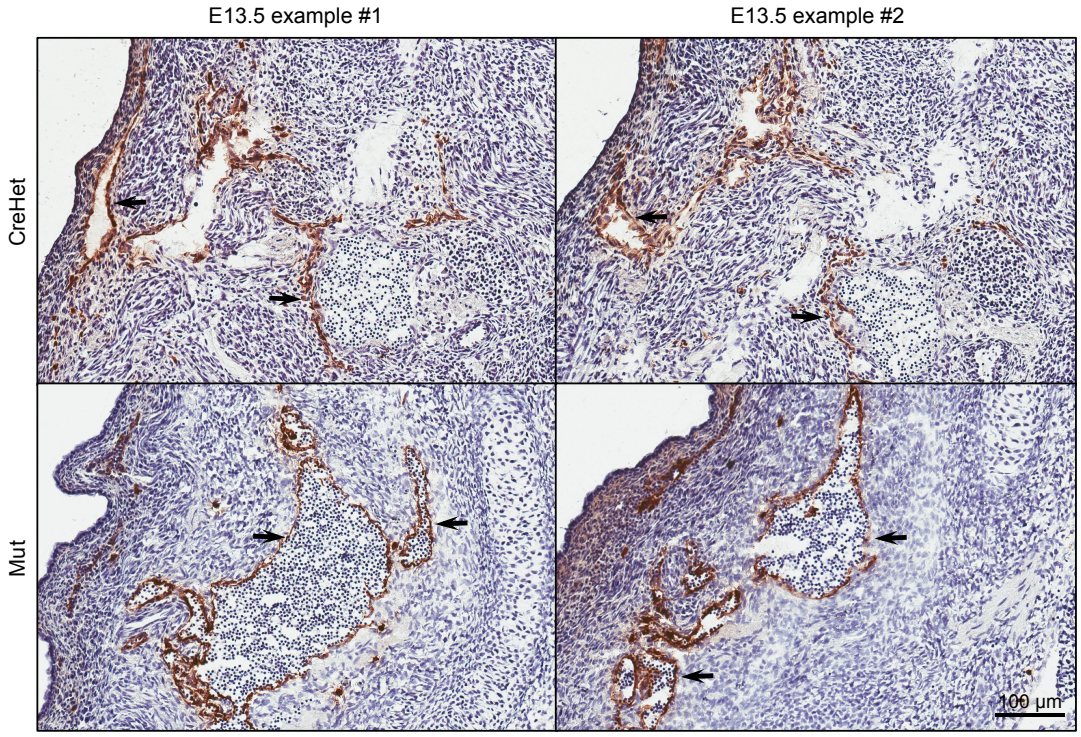

Figure S4. Endothelial *Chd1* mutants display blood within lymphatic vessels.

Immunohistochemical staining of Lyve1 marks lymphatic vessels (arrows) that appear collapsed or open but devoid of blood cells in CreHet control. These vessels are enlarged and filled with blood cells in endothelial *Chd1* mutants.

Figure S5. *Chd1* mutant hemogenic clusters express Kit.

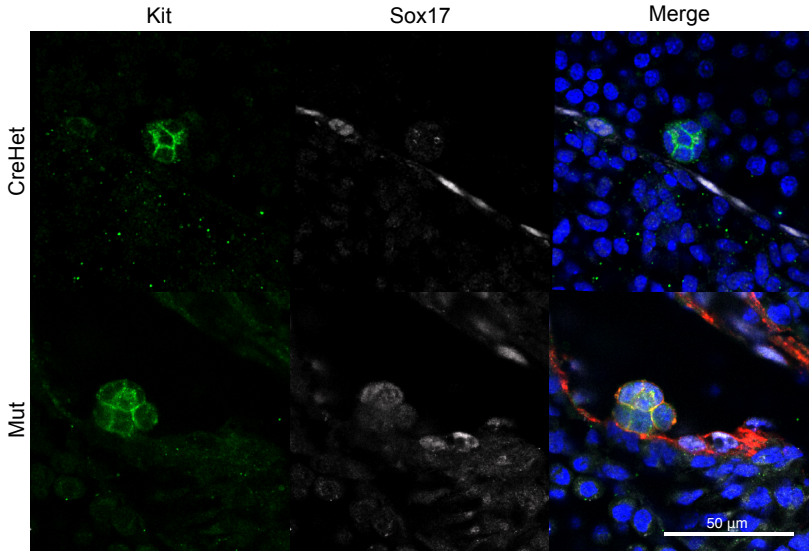

Figure S5. *Chd1* mutant hemogenic clusters express Kit.

Intra-aortic clusters in the E10.5 mutant AGM show proper expression of Kit in *Chd1* mutants.

Figure S6. Hematopoietic and growth genes are down-regulated in *Chd1* mutant endothelium.

A Immune Response genes

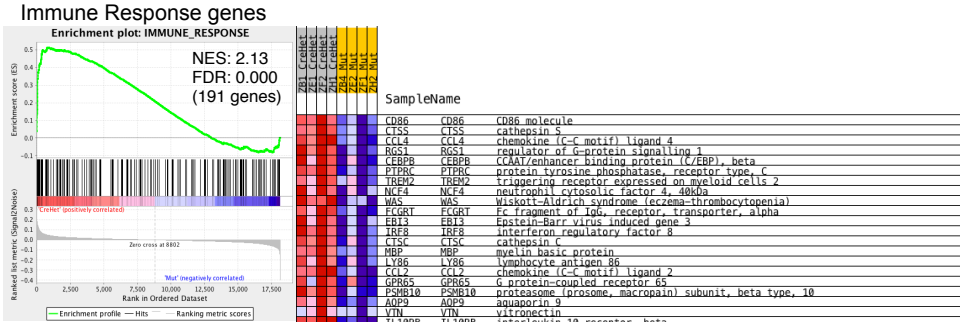

B Gata2 target genes.

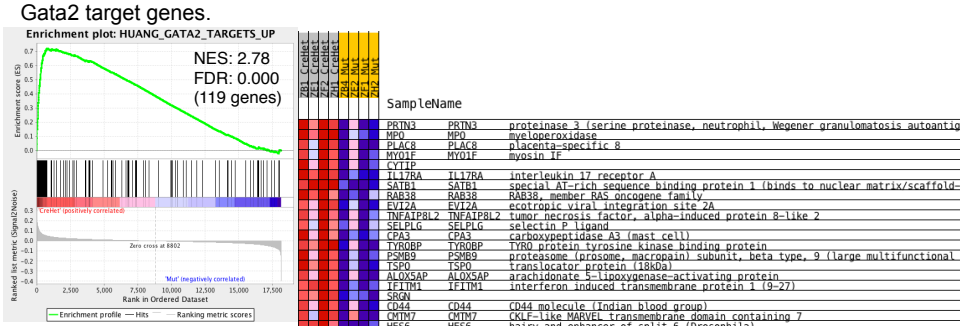

C Runx1-Runx1t1 target genes.

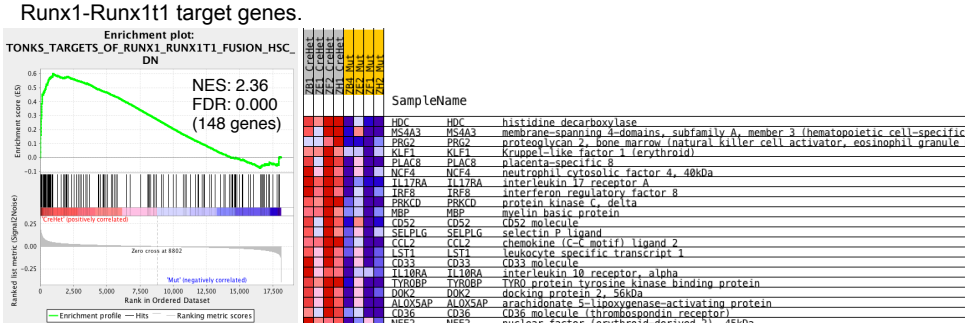

D

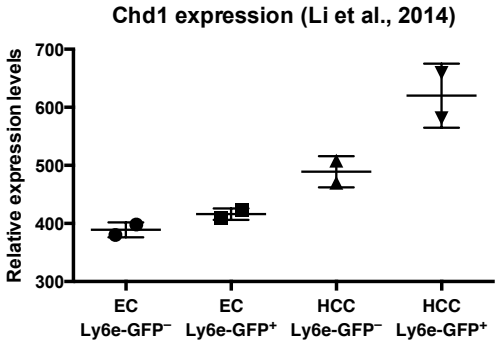

Figure S6. Hematopoietic and growth genes are down-regulated in *Chd1* mutant endothelium.

(A) GSEA for genes annotated with the GO term “Immune Response”.

(B) GSEA for genes up-regulated in G1ME cells upon knockdown of *Gata2* by RNAi. (PMID: 19620289)

(C) GSEA for genes down-regulated in normal hematopoietic progenitors by Runx1-Runx1t1 fusion. (PMID: 17898786)

(D) Microarray data from Li et al. show an elevated expression of *Chd1* in hematopoietic cluster cells (HCC) compared to endothelial cells (EC).

NES: net enrichment score. FDR: false discovery rate.

Figure S7. Myc target genes and translation-related genes are down-regulated in Chd1 mutant endothelium.

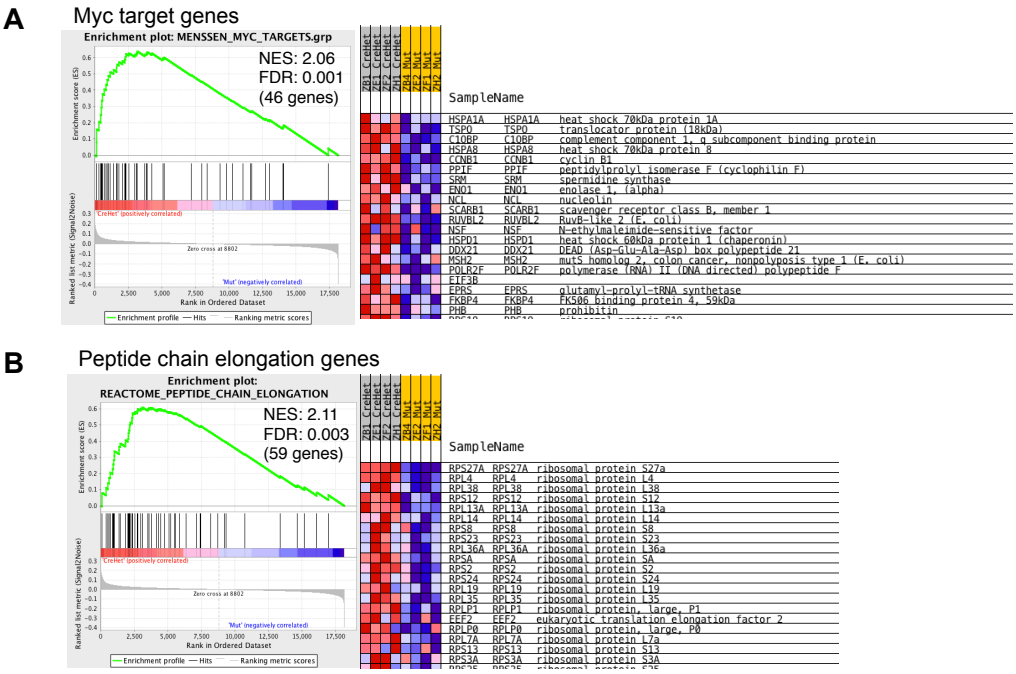

Figure S7. Myc target genes and translation-related genes are down-regulated in Chd1 mutant endothelium.

(A) GSEA for genes up-regulated by adenoviral expression of Myc in HUVEC cells. (PMID: 11983916)

(B) GSEA for genes involved in peptide chain elongation as annotated in the Reactome Pathway Database.

Table 1. Genotypes of offspring obtained from crossing *Chd1*$^{flox/flox}$ mice with *Tie2-Cre* or *Vav-Cre*

Cre line used	Stage	Total (Litters)	Genotypes				% Mut
			WT	Het	CreHet	Mut	
Tie2-Cre	E11.5	132 (18)	28	33	39	32	24.2
	E13.5	119 (16)	28	27	35	29	24.4
	E15.5	60 (9)	16	18	21	5	8.3
	Postnatal	123 (23)	54	33	36	0	0
Vav-Cre	Postnatal	165 (19)	48	38	47	32	19.4

Chapter 3

Materials and Methods

Mice

Tie2-Cre (Braren et al., 2006), *Vav-Cre* (de Boer et al., 2003), Ai14 tdTomato reporter (Madisen et al., 2010) and *Chd1* mutant mice (Guzman-Ayala et al., 2015) have been previously described. These mice were all backcrossed for at least eight generations onto a C57BL/6 genetic background. Care and use of mice were in accordance with the guidelines of the University of California, San Francisco (UCSF) Institutional Animal Care and Use Committee (IACUC). Conceptuses were generated from timed matings. Detection of the vaginal plug was considered as embryonic day (E) 0.5.

β-galactosidase staining

E13.5 embryos were fixed in 4% paraformaldehyde overnight, followed by serial overnight incubations in 10%, 20% and 30% sucrose, and frozen in Tissue-Tek OCT Compound (Sakura Finetek, 4583). 30 μm cryosections were obtained (Leica Biosystems CM3050S) and mounted on glass slides. Cryosections were incubated overnight at 37°C in X-gal staining solution [5 mM $K_3Fe(C_6FeK_3N_6)$, 5 mM $K_4Fe(C_6FeK_4N_6{\bullet}3H2O)$, 0.5 mg/ml X-gal in X-gal buffer (5mM EGTA, 2mM $MgCl_2{\bullet}6H2O$, 0.02% NP40, 0.01% deoxycholate in DPBS)]. Cryosections were counterstained with Nuclear Fast Red (Vector Labs), mounted with PolyMount (Polysciences) and imaged using the ScanScope XT slide scanner (Aperio Technologies).

Flow cytometry and cell sorting

Whole embryos, FLs, or AGMs were dissected and dissociated to single cells by treating with 1 mg/ml Collagenase Type IV (Gibco) and 0.8 mg/ml DNase I (Worthington) for 10 min at 37°C. Cells were incubated with fluorescently labeled antibodies for 60 min at 4°C, washed, and analyzed on a LSR II (BD Biosciences) or sorted on a FACSAria II (BD Biosciences). For cell cycle analyses, dissociated single cells were incubated in 10 μM EdU for 1 hour, followed by fixation and EdU detection using Click-iT EdU Flow Cytometry Kit (Molecular Probes) following the manufacturer's instructions. For total nascent RNA transcription analyses, dissociated single cells were incubated in 1 mM EU for 1 hour, followed by fixation and EU detection using Click-iT RNA Imaging Kit (Molecular Probes) following the manufacturer's protocol for flow cytometry. Data were analyzed using FlowJo software (Tree Star). Antibodies and conjugates are listed in Table S1.

RNA Isolation and Quantitative RT-PCR

Total RNA were isolated from sorted cells using Arcturus PicoPure RNA Isolation Kit (Applied Biosystems) or RNeasy Plus Micro Kit (Qiagen). cDNA was generated using High Capacity cDNA Reverse Transcriptase Kit (Applied Biosystems) and qRT-PCR reactions were performed in triplicates using the SYBR FAST ABI Prism 2X qPCR Master Mix (Kapa Biosystems) and ran on a ViiA 7 Real-Time PCR System (Applied Biosystems). Relative abundance of mRNAs was calculated using the ViiA 7 software

by normalization to *Gapdh*, *Ubb*, and *Rpl7* mRNA levels. Primer sequences are listed in Table S2.

Hematopoietic progenitor assays

CFU assays were performed using Methocult M3434 (Stem Cell Technologies), while BFU-E assays were performed using Methocult M3334 (Stem Cell Technologies). Cells were plated in duplicates in 35mm culture dishes according to the manufacturer's instructions. Plates were incubated at 37°C in a humidified chamber under 5% CO_2. Hematopoietic colonies were counted with an inverted microscope at day 3 of culture. OP9-DL1 T-lymphoid differentiation assays were performed as described (Holmes and Zúñiga-Pflücker, 2009). Dissected AGMs were dissociated into single-cell suspension prior to culture with OP9-DL1 cells. Co-cultures were passaged every 5-7 days for 5 weeks, and then harvested for flow cytometry analysis.

Immunofluorescence

E10.5 embryos were fixed in 2% paraformaldehyde solution overnight and frozen in Tissue-Tek OCT Compound (Sakura Finetek, 4583). 20-40 μm cryosections were obtained (Thermo Scientific Micron, HM550) and mounted. Slides were dried for 1 hr at room temperature, washed with PBST (0.5% Tween or Triton-X100) and incubated in blocking buffer (PBST, 1% BSA, 5% donkey serum) for 1 hr. Primary antibodies were incubated at 4°C overnight or room temperature for 6 hrs in blocking buffer. Slides were washed with PBST and incubated with the secondary antibody for 2 hrs, washed, stained with 2 ug/ul DAPI and mounted in Vectashield (H-1400). Images were captured

on a Leica SPE Confocal Microscope and compiled using Imaris 7.6 (Bitplane; Belfast, UK) software. Hematopoietic clusters were quantified by analyzing 5 serial 40 μm cryosections immediately caudal to the forelimb bud in each embryo. Clusters were defined to be groups of 4 or more DAPI$^+$ cells associated with the endothelial layer that stain positively for CD31 and Runx1. Antibodies used are listed in Table S1.

Microarray analysis

Whole genome gene expression analysis was performed on CD31$^+$ tdTomato$^+$ cells sorted from 4 littermate pairs of CreHet and mutant embryos. Total RNA was extracted using Arcturus PicoPure RNA Isolation Kit (Applied Biosystems), amplified with Ovation PicoSL WTA System V2 (NuGEN), labeled with Encore BiotinIL Module (NuGEN) and hybridized to MouseRef-8 v2.0 Expression BeadChip (Illumina) at the UCLA Neuroscience Genomics Core. Gene expression data were quantile normalized and sample heterogeneity was assessed in R with the SampleNetwork function (Oldham et al., 2012). Batch normalization was conducted using ComBat (Johnson et al., 2007) with embryo genotype as a covariate. Statistical testing was performed on log2-transformed data using the Bioconductor package linear models for microarray data (limma). Differentially expressed genes were identified by using thresholds of $p < 0.01$ and log2 fold change > 0.4 and are listed in Table S3. Microarray data have been deposited in NCBI's Gene Expression Omnibus and are accessible through GEO Series accession number GSE62796. Gene ontology analysis was conducted using DAVID (Huang et al., 2009), and the output was fed into Enrichment Map (Merico et al., 2010) for enrichment analysis using a cut-off of $p < 0.001$, FDR < 0.01 and overlap coefficient of 0.6. Gene

set enrichment analysis (GSEA) was performed as described (Subramanian et al., 2005).

Statistical analyses

All data are presented as mean ± s.e.m. and calculated using Prism 6 software (Graphpad). Chi-square tests were used to test for statistical significance in litter sizes. When comparing mutants to the other three genotypes, statistical significance was assessed using a one-way ANOVA followed by Tukey's multiple comparison tests. Unpaired two-tailed t tests were used when comparing between two categories. *, $p \leq 0.05$; **, $p \leq 0.01$; ***, $p \leq 0.001$; ****, $p \leq 0.0001$

Supplemental Table S1. List of antibodies used in this study.

Antibody	Company	Catalog	Host Isotype	Clone	Conjugate
Anti-Goat Secondary	Invitrogen	A21447	Donkey	N.A.	Alexa 647
Anti-Rabbit Secondary	Invitrogen	A21206	Donkey	N.A.	Alexa 488
Anti-Rat Secondary	Invitrogen	A21208	Donkey	N.A.	Alexa 488
Anti-Rat Secondary	Invitrogen	A21209	Donkey	N.A.	Alexa 594
CD117 (Kit)	BioLegend	105812	Rat IgG2b, κ	2B8	APC
CD117 (Kit)	BD Pharmingen	553352	Rat IgG2b, κ	2B8	N.A.
CD11b	BioLegend	101216	Rat IgG2b, κ	M1/70	PE-Cy7
CD19	BioLegend	115530	Rat IgG2a, κ	6D5	APC-Cy7
CD31 (PECAM-1)	BioLegend	102506	Rat IgG2a, κ	MEC13.3	FITC
CD31 (PECAM-1)	BioLegend	102418	Rat IgG2a, κ	390	PE-Cy7
CD31 (PECAM-1)	BD Pharmingen	553370	Rat IgG2a, κ	MEC13.3	N.A.
CD4	BioLegend	100548	Rat IgG2a, κ	RM4-5	BV605
CD45 (LCA)	BioLegend	103116	Rat IgG2b, k	30-F11	APC-Cy7
CD45 (LCA)	BioLegend	103122	Rat IgG2b, k	30-F11	Alexa 488
CD45 (LCA)	BioLegend	103114	Rat IgG2b, k	30-F11	PE-Cy7
CD45 (LCA)	BioLegend	103132	Rat IgG2b, κ	30-F11	PerCP-Cy5.5
CD8	BioLegend	100733	Rat IgG2a, κ	53-6.7	PerCP-Cy5.5
Cleaved Caspase-3	Cell Signaling	9661	Rabbit	Asp175	N.A.

Supplemental Table S1. List of antibodies used in this study. (cont'd)

Antibody	Company	Catalog	Host Isotype	Clone	Conjugate
Ly-6A/E (Sca-1)	BioLegend	108108	Rat IgG2a, κ	D7	PE
Ly-6G (Gr-1)	BD Biosciences	553127	Rat IgG2b, κ	RB6-8C5	FITC
NK1.1	BioLegend	108708	Mouse IgG2a, κ	PK136	PE
Runx1,2,3	Abcam	Ab92336	Rabbit IgG	EPR3099	N.A.
Sox17	R&D Systems	AF1924	Goat IgG	Q9H6I2	N.A.
TCRβ	BioLegend	109212	Armenian Hamster IgG	H57-597	APC
TER-119	BioLegend	116228	Rat IgG2b, κ	TER-119	PerCP-Cy5.5
TER-119	BioLegend	116208	Rat IgG2b, κ	TER-119	PE

Supplemental Table S2. List of qRT-PCR primers used in this study.

Gene	F/R	Sequence
Ubb	F	GCGGTTTGTGCTTTCATCAC
	R	GGCAAAGATCAGCCTCTGCT
L7	F	AGCGGATTGCCTTGACAGA
	R	AACTTGAAGGGCCACAGGAA
GAPDH	F	AGGTCGGTGTGAACGGATTTG
	R	TGTAGACCATGTAGTTGAGGTCA
Fabpi-200	F	TGGACAGGACTGGACCTCTGCTTTCCTAGA
	R	TAGAGCTTTGCCACATCACAGGTCATTCAG
Fabpi-500	F	CCTCCGGAGAGCAGCGATTAAAAGTGTCAG
	R	TAGAGCTTTGCCACATCACAGGTCATTCAG
Chd1-flox allele	F	CGGAACCGAAGTTCCTATTCCGAAGTTCCT
	R	CCGCCTACTGCGACTATAGAGATATCAACC
Chd1 exon15-16	F	CAAGGAGCTTGAGCCATTTC
	R	TGGTGGTTTAATGAGGTAGCAA
ζ-globin	F	TGGATTCTGTGTGGGACTAAGGC
	R	GGGCTTGGTGGGACTGTAAGG
α1/α2-globin	F	GCACAACCCAGCCCCAGAAT
	R	ACACGCCCTTGGAGCAGTTC
εγ-globin	F	CCAGACTTGCCATCATGGTGA
	R	TCACCACCAACCTCTTCAACAT
βH1-globin	F	GGACAGGTCTTCAGCCTCTTGA
	R	CAGATGCTTGTGATAGCTGCCT
β1-globin	F	CACCGAAGCCTGATTCCGTAGA
	R	GAAGCAAATGTGAGGAGCAACTGA
β2-globin	F	TGGTTGTCATCTCTGAAGCCTCAC
	R	CTGCCCACTCTGTCCTCTCTGA

References

Ahmad, K., and Henikoff, S. (2002). The histone variant H3.3 marks active chromatin by replication-independent nucleosome assembly. Mol Cell *9*, 1191–1200.

Balhorn, R. (2007). The protamine family of sperm nuclear proteins. Genome Biol *8*, 227.

Bao, S., Tang, F., Li, X., Hayashi, K., Gillich, A., Lao, K., and Surani, M.A. (2009). Epigenetic reversion of post-implantation epiblast to pluripotent embryonic stem cells. Nature *461*, 1292–1295.

Baron, M.H., Isern, J., and Fraser, S.T. (2012). The embryonic origins of erythropoiesis in mammals. Blood *119*, 4828–4837.

Barton, S.C., Arney, K.L., Shi, W., Niveleau, A., Fundele, R., Surani, M.A., and Haaf, T. (2001). Genome-wide methylation patterns in normal and uniparental early mouse embryos. Hum Mol Genet *10*, 2983–2987.

Bertrand, J.Y., Chi, N.C., Santoso, B., Teng, S., Stainier, D.Y.R., and Traver, D. (2010). Haematopoietic stem cells derive directly from aortic endothelium during development. Nature *464*, 108–111.

Bhutani, N., Brady, J.J., Damian, M., Sacco, A., Corbel, S.Y., and Blau, H.M. (2010). Reprogramming towards pluripotency requires AID-dependent DNA demethylation. Nature *463*, 1042–1047.

Blelloch, R., Wang, Z., Meissner, A., Pollard, S., Smith, A., and Jaenisch, R. (2006). Reprogramming efficiency following somatic cell nuclear transfer is influenced by the differentiation and methylation state of the donor nucleus. Stem Cells *24*, 2007–2013.

Boisset, J.-C., Clapes, T., Klaus, A., Papazian, N., Onderwater, J., Mommaas-Kienhuis, M., Cupedo, T., and Robin, C. (2014). Progressive maturation towards hematopoietic stem cells in the mouse embryo aorta. Blood.

Boisset, J.-C., van Cappellen, W., Andrieu-Soler, C., Galjart, N., Dzierzak, E., and Robin, C. (2010). In vivo imaging of haematopoietic cells emerging from the mouse aortic endothelium. Nature *464*, 116–120.

Boyer, L.A., Plath, K., Zeitlinger, J., Brambrink, T., Medeiros, L.A., Lee, T.I., Levine, S.S., Wernig, M., Tajonar, A., Ray, M.K., et al. (2006). Polycomb complexes repress developmental regulators in murine embryonic stem cells. Nat Cell Biol *441*, 349–353.

Braren, R., Hu, H., Kim, Y.H., Beggs, H.E., Reichardt, L.F., and Wang, R. (2006). Endothelial FAK is essential for vascular network stability, cell survival, and lamellipodial formation. J Cell Biol *172*, 151–162.

Braunschweig, U., Hogan, G.J., Pagie, L., and van Steensel, B. (2009). Histone H1 binding is inhibited by histone variant H3.3. Embo J *28*, 3635–3645.

Cai, S., Lee, C.C., and Kohwi-Shigematsu, T. (2006). SATB1 packages densely looped, transcriptionally active chromatin for coordinated expression of cytokine genes. Nat Genet *38*, 1278–1288.

Carter, M.G., Sharov, A.A., VanBuren, V., Dudekula, D.B., Carmack, C.E., Nelson, C., and Ko, M.S.H. (2005). Transcript copy number estimation using a mouse whole-genome oligonucleotide microarray. Genome Biol *6*, R61.

Chambers, I., Silva, J., Colby, D., Nichols, J., Nijmeijer, B., Robertson, M., Vrana, J., Jones, K., Grotewold, L., and Smith, A. (2007). Nanog safeguards pluripotency and mediates germline development. Nature *450*, 1230–1234.

Chen, M.J., Yokomizo, T., Zeigler, B.M., Dzierzak, E., and Speck, N.A. (2009). Runx1 is required for the endothelial to haematopoietic cell transition but not thereafter. Nature *457*, 887–891.

Cheng, A.M., Rowley, B., Pao, W., Hayday, A., Bolen, J.B., and Pawson, T. (1995). Syk tyrosine kinase required for mouse viability and B-cell development. Nature *378*, 303–306.

Chin, M.H., Mason, M.J., Xie, W., Volinia, S., Singer, M., Peterson, C., Ambartsumyan, G., Aimiuwu, O., Richter, L., Zhang, J., et al. (2009). Induced pluripotent stem cells and embryonic stem cells are distinguished by gene expression signatures. Cell Stem Cell *5*, 111–123.

Chow, C., Georgiou, A., Szutorisz, H., Maia e Silva, A., Pombo, A., Barahona, I., Dargelos, E., Canzonetta, C., and Dillon, N. (2005). Variant histone H3.3 marks promoters of transcriptionally active genes during mammalian cell division. EMBO Rep *6*, 354–360.

Cui, L., Johkura, K., Yue, F., Ogiwara, N., Okouchi, Y., Asanuma, K., and Sasaki, K. (2004). Spatial distribution and initial changes of SSEA-1 and other cell adhesion-related molecules on mouse embryonic stem cells before and during differentiation. J. Histochem. Cytochem. *52*, 1447–1457.

Cumano, A., and Godin, I. (2007). Ontogeny of the hematopoietic system. Annu. Rev. Immunol. *25*, 745–785.

de Boer, J., Williams, A., Skavdis, G., Harker, N., Coles, M., Tolaini, M., Norton, T., Williams, K., Roderick, K., Potocnik, A.J., et al. (2003). Transgenic mice with hematopoietic and lymphoid specific expression of Cre. Eur J Immunol *33*, 314–325.

de Bruijn, M.F., Speck, N.A., Peeters, M.C., and Dzierzak, E. (2000). Definitive hematopoietic stem cells first develop within the major arterial regions of the mouse embryo. Embo J *19*, 2465–2474.

de Bruijn, M.F.T.R., Ma, X., Robin, C., Ottersbach, K., Sanchez, M.-J., and Dzierzak, E. (2002). Hematopoietic stem cells localize to the endothelial cell layer in the midgestation mouse aorta. Immunity *16*, 673–683.

de Pater, E., Kaimakis, P., Vink, C.S., Yokomizo, T., Yamada-Inagawa, T., Van Der Linden, R., Kartalaei, P.S., Camper, S.A., Speck, N., and Dzierzak, E. (2013). Gata2 is required for HSC generation and survival. J. Exp. Med. *210*, 2843–2850.

Dobreva, G., Chahrour, M., Dautzenberg, M., Chirivella, L., Kanzler, B., Fariñas, I., Karsenty, G., and Grosschedl, R. (2006). SATB2 is a multifunctional determinant of craniofacial patterning and osteoblast differentiation. *125*, 971–986.

Dzierzak, E., and Speck, N.A. (2008). Of lineage and legacy: the development of mammalian hematopoietic stem cells. Nat Immunol *9*, 129–136.

Efroni, S., Duttagupta, R., Cheng, J., Dehghani, H., Hoeppner, D.J., Dash, C., Bazett-Jones, D.P., Le Grice, S., McKay, R.D.G., Buetow, K.H., et al. (2008). Global transcription in pluripotent embryonic stem cells. Cell Stem Cell *2*, 437–447.

Elsaesser, S.J., Goldberg, A.D., and Allis, C.D. (2010). New functions for an old variant: no substitute for histone H3.3. Curr Opin Genet Dev *20*, 110–117.

Espín-Palazón, R., Stachura, D.L., Campbell, C.A., García-Moreno, D., Del Cid, N., Kim, A.D., Candel, S., Meseguer, J., Mulero, V., and Traver, D. (2014). Proinflammatory signaling regulates hematopoietic stem cell emergence. Cell *159*, 1070–1085.

Flanagan, J.F., Mi, L.-Z., Chruszcz, M., Cymborowski, M., Clines, K.L., Kim, Y., Minor, W., Rastinejad, F., and Khorasanizadeh, S. (2005). Double chromodomains cooperate to recognize the methylated histone H3 tail. Nature *438*, 1181–1185.

Fraser, S.T., Isern, J., and Baron, M.H. (2007). Maturation and enucleation of primitive erythroblasts during mouse embryogenesis is accompanied by changes in cell-surface antigen expression. Blood *109*, 343–352.

Furusawa, T., Ohkoshi, K., Honda, C., Takahashi, S., and Tokunaga, T. (2004). Embryonic stem cells expressing both platelet endothelial cell adhesion molecule-1 and stage-specific embryonic antigen-1 differentiate predominantly into epiblast cells in a chimeric embryo. Biol Reprod *70*, 1452–1457.

Gaspar-Maia, A., Alajem, A., Polesso, F., Sridharan, R., Mason, M.J., Heidersbach, A., Ramalho-Santos, J., McManus, M.T., Plath, K., Meshorer, E., et al. (2009). Chd1 regulates open chromatin and pluripotency of embryonic stem cells. Nature *460*, 863–868.

Gkikopoulos, T., Schofield, P., Singh, V., Pinskaya, M., Mellor, J., Smolle, M., Workman, J.L., Barton, G.J., and Owen-Hughes, T. (2011). A role for Snf2-related nucleosome-spacing enzymes in genome-wide nucleosome organization. Science *333*, 1758–1760.

Goldberg, A.D., Banaszynski, L.A., Noh, K.-M., Lewis, P.W., Elsaesser, S.J., Stadler, S., Dewell, S., Law, M., Guo, X., Li, X., et al. (2010). Distinct factors control histone variant H3.3 localization at specific genomic regions. *140*, 678–691.

Grskovic, M., Chaivorapol, C., Gaspar-Maia, A., Li, H., and Ramalho-Santos, M. (2007). Systematic identification of cis-regulatory sequences active in mouse and human embryonic stem cells. PLoS Genet *3*, e145.

Guzman-Ayala, M., Sachs, M., Koh, F.M., Onodera, C., Bulut-Karslioglu, A., Lin, C.-J., Wong, P., Nitta, R., Song, J.S., and Ramalho-Santos, M. (2015). Chd1 is essential for the high transcriptional output and rapid growth of the mouse epiblast. Development. (in press)

Hajkova, P., Ancelin, K., Waldmann, T., Lacoste, N., Lange, U.C., Cesari, F., Lee, C., Almouzni, G., Schneider, R., and Surani, M.A. (2008). Chromatin dynamics during epigenetic reprogramming in the mouse germ line. Nature *452*, 877–881.

Hajkova, P., Erhardt, S., Lane, N., Haaf, T., El-Maarri, O., Reik, W., Walter, J., and Surani, M.A. (2002). Epigenetic reprogramming in mouse primordial germ cells. Mech Dev *117*, 15–23.

Hammoud, S.S., Nix, D.A., Zhang, H., Purwar, J., Carrell, D.T., and Cairns, B.R. (2009). Distinctive chromatin in human sperm packages genes for embryo development. Nature *460*, 473–478.

Hawkins, R.D., Hon, G.C., Lee, L.K., Ngo, Q.-M., Lister, R., Pelizzola, M., Edsall, L.E., Kuan, S., Luu, Y., Klugman, S., et al. (2010). Distinct epigenomic landscapes of pluripotent and lineage-committed human cells. Cell Stem Cell *6*, 479–491.

Hayashi, K., de Sousa Lopes, S.M.C., Tang, F., and Surani, M.A. (2008). Dynamic equilibrium and heterogeneity of mouse pluripotent stem cells with distinct functional and epigenetic states. Cell Stem Cell *3*, 391–401.

Ho, L., Jothi, R., Ronan, J.L., Cui, K., Zhao, K., and Crabtree, G.R. (2009a). An embryonic stem cell chromatin remodeling complex, esBAF, is an essential component of the core pluripotency transcriptional network. Proc Natl Acad Sci USA *106*, 5187–5191.

Ho, L., Ronan, J.L., Wu, J., Staahl, B.T., Chen, L., Kuo, A., Lessard, J., Nesvizhskii, A.I., Ranish, J., and Crabtree, G.R. (2009b). An embryonic stem cell chromatin remodeling complex, esBAF, is essential for embryonic stem cell self-renewal and pluripotency. Proc Natl Acad Sci USA *106*, 5181–5186.

Holmes, R., and Zúñiga-Pflücker, J.C. (2009). The OP9-DL1 system: generation of T-lymphocytes from embryonic or hematopoietic stem cells in vitro. Cold Spring Harb Protoc *2009*, pdb.prot5156–pdb.prot5156.

Hödl, M., and Basler, K. (2009). Transcription in the absence of histone H3.3. *19*, 1221–1226.

Huang, D.W., Sherman, B.T., and Lempicki, R.A. (2009). Systematic and integrative analysis of large gene lists using DAVID bioinformatics resources. Nat Protoc *4*, 44–57.

Huangfu, D., Maehr, R., Guo, W., Eijkelenboom, A., Snitow, M., Chen, A.E., and Melton, D.A. (2008). Induction of pluripotent stem cells by defined factors is greatly improved by small-molecule compounds. Nat Biotechnol *26*, 795–797.

Isern, J., He, Z., Fraser, S.T., Nowotschin, S., Ferrer-Vaquer, A., Moore, R., Hadjantonakis, A.-K., Schulz, V., Tuck, D., Gallagher, P.G., et al. (2011). Single-lineage transcriptome analysis reveals key regulatory pathways in primitive erythroid progenitors in the mouse embryo. Blood *117*, 4924–4934.

Johnson, W.E., Li, C., and Rabinovic, A. (2007). Adjusting batch effects in microarray expression data using empirical Bayes methods. Biostatistics *8*, 118–127.

Jones, P.A. (1999). The DNA methylation paradox. Trends in Genetics *15*, 34–37.

Kessler, J.D., Kahle, K.T., Sun, T., Meerbrey, K.L., Schlabach, M.R., Schmitt, E.M., Skinner, S.O., Xu, Q., Li, M.Z., Hartman, Z.C., et al. (2012). A SUMOylation-dependent transcriptional subprogram is required for Myc-driven tumorigenesis. Science *335*, 348–353.

Kingsley, P.D., Malik, J., Emerson, R.L., Bushnell, T.P., McGrath, K.E., Bloedorn, L.A., Bulger, M., and Palis, J. (2006). “Maturational” globin switching in primary primitive erythroid cells. Blood *107*, 1665–1672.

Kissa, K., and Herbomel, P. (2010). Blood stem cells emerge from aortic endothelium by a novel type of cell transition. Nature *464*, 112–115.

Konev, A.Y., Tribus, M., Park, S.Y., Podhraski, V., Lim, C.Y., Emelyanov, A.V., Vershilova, E., Pirrotta, V., Kadonaga, J.T., Lusser, A., et al. (2007). CHD1 motor protein is required for deposition of histone variant H3.3 into chromatin in vivo. Science *317*, 1087–1090.

Ku, M., Koche, R.P., Rheinbay, E., Mendenhall, E.M., Endoh, M., Mikkelsen, T.S., Presser, A., Nusbaum, C., Xie, X., Chi, A.S., et al. (2008). Genomewide analysis of PRC1 and PRC2 occupancy identifies two classes of bivalent domains. PLoS Genet *4*, e1000242.

Kumano, K., Chiba, S., Kunisato, A., Sata, M., Saito, T., Nakagami-Yamaguchi, E., Yamaguchi, T., Masuda, S., Shimizu, K., Takahashi, T., et al. (2003). Notch1 but not Notch2 is essential for generating hematopoietic stem cells from endothelial cells. Immunity *18*, 699–711.

Latham, K.E., Solter, D., and Schultz, R.M. (1992). Acquisition of a transcriptionally permissive state during the 1-cell stage of mouse embryogenesis. Dev Biol *149*, 457–462.

Laurent, L., Wong, E., Li, G., Huynh, T., Tsirigos, A., Ong, C.T., Low, H.M., Kin Sung, K.W., Rigoutsos, I., Loring, J., et al. (2010). Dynamic changes in the human methylome during differentiation. Genome Res *20*, 320–331.

Lee, J., Inoue, K., Ono, R., Ogonuki, N., Kohda, T., Kaneko-Ishino, T., Ogura, A., and Ishino, F. (2002). Erasing genomic imprinting memory in mouse clone embryos produced from day 11.5 primordial germ cells. Development *129*, 1807–1817.

Leeb, M., Pasini, D., Novatchkova, M., Jaritz, M., Helin, K., and Wutz, A. (2010). Polycomb complexes act redundantly to repress genomic repeats and genes. Genes Dev *24*, 265–276.

Levey, I.L., Stull, G.B., and Brinster, R.L. (1978). Poly(A) and synthesis of polyadenylated RNA in the preimplantation mouse embryo. Dev Biol *64*, 140–148.

Li, Y., Esain, V., Teng, L., Xu, J., Kwan, W., Frost, I.M., Yzaguirre, A.D., Cai, X., Cortes, M., Maijenburg, M.W., et al. (2014). Inflammatory signaling regulates embryonic hematopoietic stem and progenitor cell production. Genes Dev *28*, 2597–2612.

Lim, K.-C., Hosoya, T., Brandt, W., Ku, C.-J., Hosoya-Ohmura, S., Camper, S.A., Yamamoto, M., and Engel, J.D. (2012). Conditional Gata2 inactivation results in HSC loss and lymphatic mispatterning. J. Clin. Invest. *122*, 3705–3717.

Lin, C.Y., Lovén, J., Rahl, P.B., Paranal, R.M., Burge, C.B., Bradner, J.E., Lee, T.I., and Young, R.A. (2012). Transcriptional amplification in tumor cells with elevated c-Myc. Cell *151*, 56–67.

Lin, J.J., Lehmann, L.W., Bonora, G., Sridharan, R., Vashisht, A.A., Tran, N., Plath, K., Wohlschlegel, J.A., and Carey, M. (2011). Mediator coordinates PIC assembly with recruitment of CHD1. Genes Dev *25*, 2198–2209.

Lister, R., Pelizzola, M., Dowen, R.H., Hawkins, R.D., Hon, G.C., Tonti-Filippini, J., Nery, J.R., Lee, L., Ye, Z., Ngo, Q.-M., et al. (2009). Human DNA methylomes at base resolution show widespread epigenomic differences. Nature *462*, 315–322.

Madisen, L., Zwingman, T.A., Sunkin, S.M., Oh, S.W., Zariwala, H.A., Gu, H., Ng, L.L., Palmiter, R.D., Hawrylycz, M.J., Jones, A.R., et al. (2010). A robust and high-throughput Cre reporting and characterization system for the whole mouse brain. Nat. Neurosci. *13*, 133–140.

Maherali, N., Sridharan, R., Xie, W., Utikal, J., Eminli, S., Arnold, K., Stadtfeld, M., Yachechko, R., Tchieu, J., Jaenisch, R., et al. (2007). Directly reprogrammed fibroblasts show global epigenetic remodeling and widespread tissue contribution. Cell Stem Cell *1*, 55–70.

Meissner, A., Wernig, M., and Jaenisch, R. (2007). Direct reprogramming of genetically unmodified fibroblasts into pluripotent stem cells. Nat Biotechnol *25*, 1177–1181.

Merico, D., Isserlin, R., Stueker, O., Emili, A., and Bader, G.D. (2010). Enrichment Map: A Network-Based Method for Gene-Set Enrichment Visualization and Interpretation. PLoS ONE *5*, e13984.

Meshorer, E., Yellajoshula, D., George, E., Scambler, P.J., Brown, D.T., and Misteli, T. (2006). Hyperdynamic plasticity of chromatin proteins in pluripotent embryonic stem cells. Dev Cell *10*, 105–116.

Mikkelsen, T.S., Hanna, J., Zhang, X., Ku, M., Wernig, M., Schorderet, P., Bernstein, B.E., Jaenisch, R., Lander, E.S., and Meissner, A. (2008). Dissecting direct reprogramming through integrative genomic analysis. Nature *454*, 49–55.

Mikkelsen, T.S., Ku, M., Jaffe, D.B., Issac, B., Lieberman, E., Giannoukos, G., Alvarez, P., Brockman, W., Kim, T.-K., Koche, R.P., et al. (2007). Genome-wide maps of chromatin state in pluripotent and lineage-committed cells. Nature *448*, 553–560.

Mito, Y., Henikoff, J.G., and Henikoff, S. (2005). Genome-scale profiling of histone H3.3 replacement patterns. Nat Genet *37*, 1090–1097.

Nie, Z., Hu, G., Wei, G., Cui, K., Yamane, A., Resch, W., Wang, R., Green, D.R., Tessarollo, L., Casellas, R., et al. (2012). c-Myc is a universal amplifier of expressed genes in lymphocytes and embryonic stem cells. Cell *151*, 68–79.

O'Carroll, D., Erhardt, S., Pagani, M., Barton, S.C., Surani, M.A., and Jenuwein, T. (2001). The polycomb-group gene Ezh2 is required for early mouse development. Mol Cell Biol *21*, 4330–4336.

Okada, Y., Yamagata, K., Hong, K., Wakayama, T., and Zhang, Y. (2010). A role for the elongator complex in zygotic paternal genome demethylation. Nature *463*, 554–558.

Oldham, M.C., Langfelder, P., and Horvath, S. (2012). Network methods for describing sample relationships in genomic datasets: application to Huntington's disease. BMC Syst Biol *6*, 63.

Ooi, S.K.T., and Bestor, T.H. (2008). The colorful history of active DNA demethylation. *133*, 1145–1148.

Oswald, J., Engemann, S., Lane, N., Mayer, W., Olek, A., Fundele, R., Dean, W., Reik, W., and Walter, J. (2000). Active demethylation of the paternal genome in the mouse zygote. *10*, 475–478.

Padrón-Barthe, L., Temiño, S., Villa Del Campo, C., Carramolino, L., Isern, J., and Torres, M. (2014). Clonal analysis identifies hemogenic endothelium as the source of the blood-endothelial common lineage in the mouse embryo. Blood *124*, 2523–2532.

Palis, J., Robertson, S., Kennedy, M., Wall, C., and Keller, G. (1999). Development of erythroid and myeloid progenitors in the yolk sac and embryo proper of the mouse. Development *126*, 5073–5084.

Paul, J., Conkie, D., and Freshney, R.I. (1972). Effect of erythropoietin on haemoglobin synthesis and haem synthesizing enzymes of mouse foetal liver cells in culture. J Embryol Exp Morphol *27*, 525–532.

Peng, J.C., Valouev, A., Swigut, T., Zhang, J., Zhao, Y., Sidow, A., and Wysocka, J. (2009). Jarid2/Jumonji coordinates control of PRC2 enzymatic activity and target gene occupancy in pluripotent cells. *139*, 1290–1302.

Persson, J., and Ekwall, K. (2010). Chd1 remodelers maintain open chromatin and regulate the epigenetics of differentiation. Exp. Cell Res. *316*, 1316–1323.

Popp, C., Dean, W., Feng, S., Cokus, S.J., Andrews, S., Pellegrini, M., Jacobsen, S.E., and Reik, W. (2010). Genome-wide erasure of DNA methylation in mouse primordial germ cells is affected by AID deficiency. Nature *463*, 1101–1105.

Puschendorf, M., Terranova, R., Boutsma, E., Mao, X., Isono, K.-I., Brykczynska, U., Kolb, C., Otte, A.P., Koseki, H., Orkin, S.H., et al. (2008). PRC1 and Suv39h specify parental asymmetry at constitutive heterochromatin in early mouse embryos. Nat Genet *40*, 411–420.

Quan, T.K., and Hartzog, G.A. (2010). Histone H3K4 and K36 methylation, Chd1 and Rpd3S oppose the functions of Saccharomyces cerevisiae Spt4-Spt5 in transcription. Genetics *184*, 321–334.

Rai, K., Huggins, I.J., James, S.R., Karpf, A.R., Jones, D.A., and Cairns, B.R. (2008). DNA demethylation in zebrafish involves the coupling of a deaminase, a glycosylase, and gadd45. *135*, 1201–1212.

Ramalho-Santos, M. (2009). iPS cells: insights into basic biology. *138*, 616–618.

Ramalho-Santos, M., Yoon, S., Matsuzaki, Y., Mulligan, R.C., and Melton, D.A. (2002). “Stemness”: transcriptional profiling of embryonic and adult stem cells. Science *298*, 597–600.

Resnick, J.L., Bixler, L.S., Cheng, L., and Donovan, P.J. (1992). Long-term proliferation of mouse primordial germ cells in culture. Nature *359*, 550–551.

Ruiz-Herguido, C., Guiu, J., D'Altri, T., Inglés-Esteve, J., Dzierzak, E., Espinosa, L., and Bigas, A. (2012). Hematopoietic stem cell development requires transient Wnt/β-catenin activity. J. Exp. Med. *209*, 1457–1468.

Sachs, M., Onodera, C., Blaschke, K., Ebata, K.T., Song, J.S., and Ramalho-Santos, M. (2013). Bivalent chromatin marks developmental regulatory genes in the mouse embryonic germline in vivo. Cell Rep *3*, 1777–1784.

Sakai, A., Schwartz, B.E., Goldstein, S., and Ahmad, K. (2009). Transcriptional and developmental functions of the H3.3 histone variant in Drosophila. *19*, 1816–1820.

Saleque, S., Cameron, S., and Orkin, S.H. (2002). The zinc-finger proto-oncogene Gfi-1b is essential for development of the erythroid and megakaryocytic lineages. Genes Dev *16*, 301–306.

Sasaki, H., and Matsui, Y. (2008). Epigenetic events in mammalian germ-cell development: reprogramming and beyond. Nat Rev Genet *9*, 129–140.

Savarese, F., Dávila, A., Nechanitzky, R., La Rosa-Velazquez, de, I., Pereira, C.F., Engelke, R., Takahashi, K., Jenuwein, T., Kohwi-Shigematsu, T., Fisher, A.G., et al. (2009). Satb1 and Satb2 regulate embryonic stem cell differentiation and Nanog expression. Genes Dev *23*, 2625–2638.

Sawamiphak, S., Kontarakis, Z., and Stainier, D.Y.R. (2014). Interferon Gamma Signaling Positively Regulates Hematopoietic Stem Cell Emergence. Dev Cell *31*, 640–653.

Schmitt, T.M., de Pooter, R.F., Gronski, M.A., Cho, S.K., Ohashi, P.S., and Zúñiga-Pflücker, J.C. (2004). Induction of T cell development and establishment of T cell competence from embryonic stem cells differentiated in vitro. Nat Immunol *5*, 410–417.

Schultz, R.M. (2002). The molecular foundations of the maternal to zygotic transition in the preimplantation embryo. Hum Reprod Update *8*, 323–331.

Schwartz, B.E., and Ahmad, K. (2005). Transcriptional activation triggers deposition and removal of the histone variant H3.3. Genes Dev *19*, 804–814.

Seki, Y., Yamaji, M., Yabuta, Y., Sano, M., Shigeta, M., Matsui, Y., Saga, Y., Tachibana, M., Shinkai, Y., and Saitou, M. (2007). Cellular dynamics associated with the genome-wide epigenetic reprogramming in migrating primordial germ cells in mice. Development *134*, 2627–2638.

Shen, X., Kim, W., Fujiwara, Y., Simon, M.D., Liu, Y., Mysliwiec, M.R., Yuan, G.-C., Lee, Y., and Orkin, S.H. (2009). Jumonji modulates polycomb activity and self-renewal versus differentiation of stem cells. *139*, 1303–1314.

Simic, R., Lindstrom, D.L., Tran, H.G., Roinick, K.L., Costa, P.J., Johnson, A.D., Hartzog, G.A., and Arndt, K.M. (2003). Chromatin remodeling protein Chd1 interacts with transcription elongation factors and localizes to transcribed genes. Embo J *22*, 1846–1856.

Simonsson, S., and Gurdon, J. (2004). DNA demethylation is necessary for the epigenetic reprogramming of somatic cell nuclei. Nat Cell Biol *6*, 984–990.

Sims, R.J., Chen, C.-F., Santos-Rosa, H., Kouzarides, T., Patel, S.S., and Reinberg, D. (2005). Human but not yeast CHD1 binds directly and selectively to histone H3 methylated at lysine 4 via its tandem chromodomains. J Biol Chem *280*, 41789–41792.

Sims, R.J., Millhouse, S., Chen, C.-F., Lewis, B.A., Erdjument-Bromage, H., Tempst, P., Manley, J.L., and Reinberg, D. (2007). Recognition of trimethylated histone H3 lysine 4 facilitates the recruitment of transcription postinitiation factors and pre-mRNA splicing. Mol Cell *28*, 665–676.

Skene, P.J., Hernandez, A.E., Groudine, M., and Henikoff, S. (2014). The nucleosomal barrier to promoter escape by RNA polymerase II is overcome by the chromatin remodeler Chd1. Elife *3*, e02042.

Smolle, M., Venkatesh, S., Gogol, M.M., Li, H., Zhang, Y., Florens, L., Washburn, M.P., and Workman, J.L. (2012). Chromatin remodelers Isw1 and Chd1 maintain chromatin structure during transcription by preventing histone exchange. Nat Struct Mol Biol *19*, 884–892.

Sridharan, R., Tchieu, J., Mason, M.J., Yachechko, R., Kuoy, E., Horvath, S., Zhou, Q., and Plath, K. (2009). Role of the murine reprogramming factors in the induction of pluripotency. *136*, 364–377.

Srinivasan, R.S., Dillard, M.E., Lagutin, O.V., Lin, F.-J., Tsai, S., Tsai, M.-J., Samokhvalov, I.M., and Oliver, G. (2007). Lineage tracing demonstrates the venous origin of the mammalian lymphatic vasculature. Genes Dev *21*, 2422–2432.

Stokes, D.G., Tartof, K.D., and Perry, R.P. (1996). CHD1 is concentrated in interbands and puffed regions of Drosophila polytene chromosomes. Proc Natl Acad Sci USA *93*, 7137–7142.

Subramanian, A., Tamayo, P., Mootha, V.K., Mukherjee, S., Ebert, B.L., Gillette, M.A., Paulovich, A., Pomeroy, S.L., Golub, T.R., Lander, E.S., et al. (2005). Gene set enrichment analysis: a knowledge-based approach for interpreting genome-wide expression profiles. Proc Natl Acad Sci USA *102*, 15545–15550.

Swiers, G., Rode, C., Azzoni, E., and de Bruijn, M.F.T.R. (2013). A short history of hemogenic endothelium. Blood Cells Mol. Dis. *51*, 206–212.

Takahashi, K., and Yamanaka, S. (2006). Induction of pluripotent stem cells from mouse embryonic and adult fibroblast cultures by defined factors. *126*, 663–676.

Teng, T., Thomas, G., and Mercer, C.A. (2013). Growth control and ribosomopathies. Curr Opin Genet Dev *23*, 63–71.

Torres-Padilla, M.-E., Bannister, A.J., Hurd, P.J., Kouzarides, T., and Zernicka-Goetz, M. (2006). Dynamic distribution of the replacement histone variant H3.3 in the mouse oocyte and preimplantation embryos. Int J Dev Biol *50*, 455–461.

Toyooka, Y., Shimosato, D., Murakami, K., Takahashi, K., and Niwa, H. (2008). Identification and characterization of subpopulations in undifferentiated ES cell culture. Development *135*, 909–918.

Turner, M., Mee, P.J., Costello, P.S., Williams, O., Price, A.A., Duddy, L.P., Furlong, M.T., Geahlen, R.L., and Tybulewicz, V.L. (1995). Perinatal lethality and blocked B-cell development in mice lacking the tyrosine kinase Syk. Nature *378*, 298–302.

Uhrin, P., Zaujec, J., Breuss, J.M., Olcaydu, D., Chrenek, P., Stockinger, H., Fuertbauer, E., Moser, M., Haiko, P., Fässler, R., et al. (2010). Novel function for blood platelets and podoplanin in developmental separation of blood and lymphatic circulation. Blood *115*, 3997–4005.

van der Heijden, G.W., Dieker, J.W., Derijck, A.A.H.A., Muller, S., Berden, J.H.M., Braat, D.D.M., van der Vlag, J., and de Boer, P. (2005). Asymmetry in histone H3 variants and lysine methylation between paternal and maternal chromatin of the early mouse zygote. Mech Dev *122*, 1008–1022.

Voncken, J.W., Roelen, B.A.J., Roefs, M., de Vries, S., Verhoeven, E., Marino, S., Deschamps, J., and van Lohuizen, M. (2003). Rnf2 (Ring1b) deficiency causes gastrulation arrest and cell cycle inhibition. Proc Natl Acad Sci USA *100*, 2468–2473.

Walker, E., Chang, W.Y., Hunkapiller, J., Cagney, G., Garcha, K., Torchia, J., Krogan, N.J., Reiter, J.F., and Stanford, W.L. (2010). Polycomb-like 2 associates with PRC2 and regulates transcriptional networks during mouse embryonic stem cell self-renewal and differentiation. Cell Stem Cell *6*, 153–166.

Wang, D., Feng, J., Wen, R., Marine, J.C., Sangster, M.Y., Parganas, E., Hoffmeyer, A., Jackson, C.W., Cleveland, J.L., Murray, P.J., et al. (2000). Phospholipase Cgamma2 is essential in the functions of B cell and several Fc receptors. Immunity *13*, 25–35.

Wang, J., Mager, J., Schnedier, E., and Magnuson, T. (2002). The mouse PcG gene eed is required for Hox gene repression and extraembryonic development. Mamm Genome *13*, 493–503.

Ward, W.S. (1991). DNA packaging and organization in mammalian spermatozoa: comparison with somatic cells. Biol Reprod *44*, 569–574.

Wykes, S., and Krawetz, S. (2003). The structural organization of sperm chromatin. J Biol Chem *278*, 29471–29477.

Yabuta, Y., Kurimoto, K., Ohinata, Y., Seki, Y., and Saitou, M. (2006). Gene expression dynamics during germline specification in mice identified by quantitative single-cell gene expression profiling. Biol Reprod *75*, 705–716.

Zape, J.P., and Zovein, A.C. (2011). Hemogenic endothelium: origins, regulation, and implications for vascular biology. Semin. Cell Dev. Biol. *22*, 1036–1047.

Zovein, A.C., Hofmann, J.J., Lynch, M., French, W.J., Turlo, K.A., Yang, Y., Becker, M.S., Zanetta, L., Dejana, E., Gasson, J.C., et al. (2008). Fate tracing reveals the endothelial origin of hematopoietic stem cells. Cell Stem Cell *3*, 625–636.

Publishing Agreement

It is the policy of the University to encourage the distribution of all theses, dissertations, and manuscripts. Copies of all UCSF theses, dissertations, and manuscripts will be routed to the library via the Graduate Division. The library will make all theses, dissertations, and manuscripts accessible to the public and will preserve these to the best of their abilities, in perpetuity.

I hereby grant permission to the Graduate Division of the University of California, San Francisco to release copies of my thesis, dissertation, or manuscript to the Campus Library to provide access and preservation, in whole or in part, in perpetuity.

Author Signature

Dec 15, 2014

Date